Spin-orbitronics using heavy or light elements

Masashi Shiraishi

Kyoto University
Japan.

Contents

/ Introduction

/ Spin-orbitronics using Bi-related heavy materials

// Bi on YIG

// Bi/Ag on YIG

// Bi-based topological insulators

/ Spin-orbitronics using nano-carbon materials

// Single-layer graphene (SLG)

// Single-walled carbon nanotubes (SWNTs)

/ Summary

Nano spin conversion

Acknowledgements

Dr. Yuichiro Ando, Dr. S. Dushenko, R. Ohshima (Kyoto U.)

// Bi on YIG

Prof. Y. Fuseya (Univ. Electrocommunications)
Dr. G. Eguchi (TU-Wien)
H. Emoto (Osaka U. & Kyoto U.⇒Denso)

// Bi/Ag on YIG

M. Matsushima (Kyoto U.)

// Bi-based topological insulators

Prof. Yoichi Ando(Osaka U. & Univ. Koeln)

// Single-layer graphene (SLG)

Prof. H. Ago (Kyushu U.)
Prof. T. Takenobu (Waseda U. & Nagoya U.)
Prof. S. Kuwabata (Osaka U.)
A. Sakai (Osaka U.)

// Single-walled carbon nanotubes (SWNTs)

Dr. H. Kataura, Dr. T. Tanaka(AIST)
E. Shigematsu & H. Nagano (Kyoto U.)

Introduction

Periodic table and the spin-orbit interaction

Nano spin conversion

元素の周期表
The Periodic Table

周期＼族	1	2	3	4	5	6	7	8	9	10	11	12	13	14	15	16	17	18
1	1 H 水素 Hydrogen 1.00794																	2 He ヘリウム Helium 4.0026
2	3 Li リチウム Lithium 6.941	4 Beryl 9.01218											5 B 硼(ホウ)素 Boron 10.811	6 C 炭素 Carbon 12.0107	7 N 窒素 Nitrogen 14.0067	8 O 酸素 Oxygen 15.9994	9 F 弗(フッ)素 Fluorine 18.9984	10 Ne ネオン Neon 20.1797
3	11 Na ナトリウム Sodium 22.9898	12 Mg マグネシウム Magnesium 24.305											13 Al アルミニウム Aluminum 26.9815	14 Si 珪(ケイ)素 Silicon 28.0855	15 P 燐(リン) Phosphorus 30.9738	16 S 硫黄 Sulfur 32.065	17 Cl 塩素 Chlorine 35.453	18 Ar アルゴン Argon 39.948
4	19 K カリウム Potassium 39.0983	20 Ca カルシウム Calcium 40.078	21 Sc スカンジウム Scandium 44.9559	22 Ti チタン Titanium 47.867	23 V バナジウム Vanadium 50.9415	24 C クロム Chromium 51.9961	Manganese 54.938	55.8			29 Cu	30 Zn 亜鉛 Zinc	31 Ga ガリウム Gallium 69.723	32 Ge ゲルマニウム Germanium 72.64	33 As 砒(ヒ)素 Arsenic 74.9216	34 Se セレン Selenium 78.96	35 Br 臭素 Bromine 79.904	36 Kr クリプトン Krypton 83.798
5	37 Rb ルビジウム Rubidium 85.4678	38 Sr ストロンチウム Strontium 87.62	39 Y イットリウム Yttrium 88.9059	40 Zr ジルコニウム Zirconium 91.224	41 Nb ニオブ Niobium 92.9064	42 Mo モリブデン Molybdenum 95.96	43 Tc テクネチウム Technetium [99]	44 Ru ルテニウム Ruthenium 101.07	ロジウム Rhodium 102.906	Pallad 106.42			In	50 Sn 錫(ス	51 Sb アンチモン Antimony 21.760	52 Te テルル Tellurium 127.60	53 I 沃(ヨウ)素 Iodine 126.904	54 Xe キセノン Xenon 131.293
6	55 Cs セシウム Cesium 132.905	56 Ba バリウム Barium 137.327	※1	72 Hf ハフニウム Hafnium 178.49	73 Ta タンタル Tantalum 180.948	74 W タングステン Tungsten 183.84	75 Re レニウム Rhenium 186.207	76 Os オスミウム Osmium 190.23	77 Ir イリジウム Iridium 192.217	78 Pt 白金(プラチナ Platinum 195.084	79 Au 金 Gold 196.967	水銀 Mercury 200.59	204.383		Bi マス h .98	84 Po ポロニウム Polonium [210]	85 At アスタチン Astatine [210]	86 Rn ラドン Radon [222]
7	87 Fr フランシウム Francium [223]	88 Ra ラジウム Radium [226]	※2	104 Rf ラザホージウム Rutherfordium [267]	105 Db ドブニウム Dubnium [268]	106 Sg シーボーギウム Seaborgium [271]	107 Bh ボーリウム Bohrium [272]	108 Hs ハッシウム Hassium [277]	109 Mt マイトネリウム Meitnerium [276]	110 Ds ダームスタチウム Darmstadtium [281]	111 Rg レントゲニウム Roentgenium [280]	112 Cn コペルニシウム Copernicium [285]	113 ? ? ? [284]	フレロビウム Flerovium [289]	115 ? ? ? [288]	116 Lv リバモリウム Livermorium [293]	117 ? ? ? [294]	118 ? ? ? [294]

※1 ランタノイド系	57 La ランタン Lanthanum 138.906	58 Ce セリウム Cerium 140.116	59 Pr プラセオジム Praseodymium 140.908	60 Nd ネオジム Neodymium 144.242	61 Pm プロメチウム Promethium [145]	62 Sm サマリウム Samarium 150.36	63 Eu ユウロピウム Europium 151.964	64 Gd ガドリニウム Gadolinium 157.25	65 Tb テルビウム Terbium 158.925	66 Dy ジスプロシウム Dysprosium 162.5	67 Ho ホルミウム Holmium 164.93	68 Er エルビウム Erbium 167.259	69 Tm ツリウム Thulium 168.934	70 Yb イッテルビウム Ytterbium 173.054	71 Lu ルテチウム Lutetium 174.967
※2 アクチノイド系	89 Ac アクチニウム Actinium [227]	90 Th トリウム Thorium 232.038	91 Pa プロトアクチニウム Protactinium 231.036	92 U ウラン Uranium 238.029	93 Np ネプツニウム Neptunium [237]	94 Pu プルトニウム Plutonium [239]	95 Am アメリシウム Americium [243]	96 Cm キュリウム Curium [247]	97 Bk バークリウム Berkelium [247]	98 Cf カリホルニウム Californium [252]	99 Es アインスタイニウム Einsteinium [252]	100 Fm フェルミウム Fermium [257]	101 Md メンデレビウム Mendelevium [258]	102 No ノーベリウム Nobelium [259]	103 Lr ローレンシウム Lawrencium [262]

Introduction

Spin-orbitronics

/ "Spin" + "Orbit" degrees of freedom

/ SOI-induced effects

Spin Hall, Rashba, Dresselhaus, Edelstein,…

/ Inversion symmetry breaking (lattice, spatial,..)

1. Heavy element
2. Bilayer system
3. Compound materials

Appropriate stages for spin-orbitronics

1. Heavy element (Large SOI)
   Bi, Pt, Ta, W, …

2. Bilayer system (Spatial inv. symmetry)
   Bi/Ag, Bi/Cu, SLG/YIG, …
   Topological insulator (vacuum/TI)

3. Compound materials(Lattice inv. symmetry)
   III-V, oxide heterostructure

Bismuth (Bi)

Bi/YIG

H. Emoto, M.S. et al., JAP 2012.

Ibid., PRB in press.

Bi/Ag/YIG

M. Matsushima, M.S. et al., in prep.

Attractive of Bismuth

Nano spin conversion

Bismuth : Group-V, a single element material.

/ Semi-metal (band overlap : 38 meV)
/ Dirac-like linear band structure
/ A small band-gap at L-point (10 meV)
/ A wide variety of attractive physics, firstly found.

the Seebeck effect (1822)
the Nernst-Ettingshausen effect (1886)
the Schbnikov-de Haas oscillation (1930)
the de Haas-van Alphen effect (1930)…..

One of the most intensively studied material in solid state physics !
(from 19th century !!)

Attractive of Bismuth for spintronics

From a spintronic viewpoint,

/ A large spin-orbit interaction (1.8 eV) !!

/ Dirac-like linear band structure

⇒ Bi garners much attention in spintronics !!

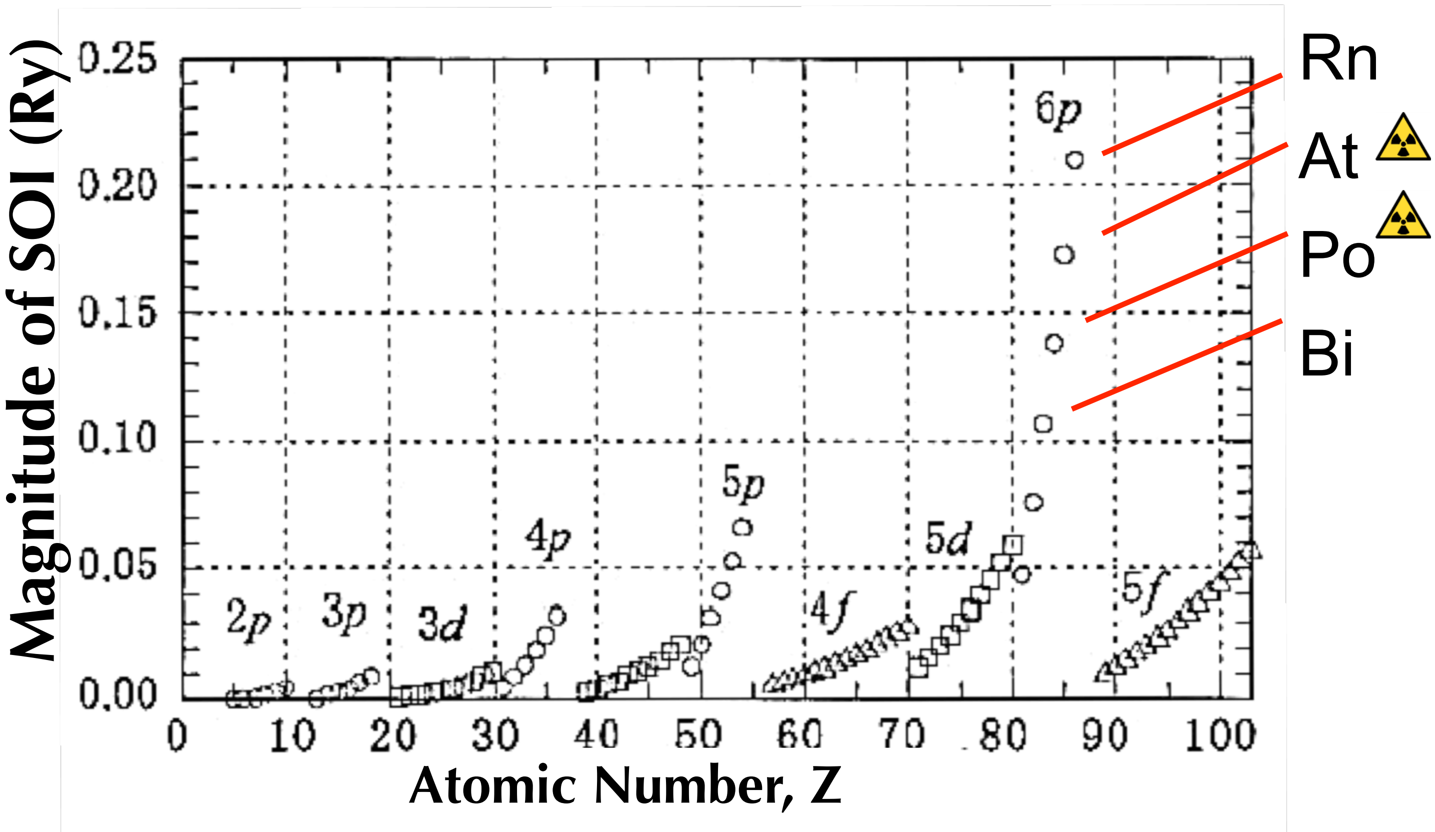

Y. Yanase and H. Harima, Kotai-Butsuri **46**, 229 (2011).

Spin conversion in Bi

Nano spin conversion

The inverse spin Hall effect (ISHE):

a-Bi*: θ_{SHE}=0.02, λ_S=8 nm (**Pt: θ_{SHE}=0.1, λ_S=7.3 nm)

*H. Emoto, M.S. et al., JAP 115 ,17C507 (2014).

D. Hou et al., APL 2012. θ_{SHE}=+0.02 & -0.07 !!

**H. L. Wang, et al., PRL 112, 197201 (2014).

poly-crystalline : λ_S ~ 20 nm (H. Emoto et al., PRB, in press.)

single crystal Bi : NO REPORT

The inverse Rashba-Edelstein effect (IREE):

A spin conversion due to the Rashba field in a 2D system.

Rashba splitting in a Bi-based system

C. Ast et al., PRL 2007.

TABLE I. Selected materials and parameters characterizing the spin splitting: Rashba energy of split states E_R, wave number offset k_0, and Rashba parameter α_R.

Material	E_R (meV)	k_0 (Å^{-1})	α_R (eV Å)	Reference
InGaAs/InAlAs heterostructure	<1	0.028	0.07	[4]
Ag(111) surface state	<0.2	0.004	0.03	[5,6]
Au(111) surface state	2.1	0.012	0.33	[6,7]
Bi(111) surface state	~ 14	~ 0.05	~ 0.56	[8]
Bi/Ag(111) surface alloy	200	0.13	3.05	This work

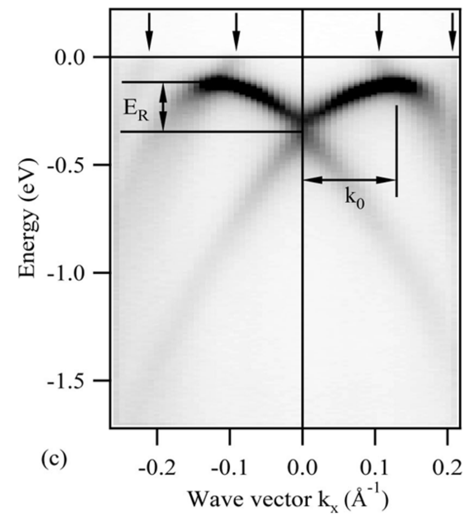

(c)

V.M. Edelstein, SSC 1990.

Solid State Communications, Vol. 73, No. 3, pp. 233–235, 1990.
Printed in Great Britain.

SPIN POLARIZATION OF CONDUCTION ELECTRONS INI
TWO-DIMENSIONAL ASYMMETRIC ELE

V.M. Edelstein

USSR Academy of Sciences, Institute of Solid State Physic

(*Received* 11 *August* 1989 *by V.M. A*

THE SYMMETRY of some two-dimensional electron systems (quantum wells, inversion layers or geterojunctions) is known to be broken with respect to reflection in plane of structure. In other words, the two normals opposite-directed to such electron layers are not equivalent. Attention to this fact was for the first time called in paper [1]. Because of absence of "up-down" symmetry an additional spin-orbit term in the effective 2D-Hamiltonian is permitted [2]

$$H_{SO} = \frac{\alpha}{\hbar}[\mathbf{pc}]\boldsymbol{\sigma}, \qquad (1)$$

where $\mathbf{p}$ is the electron momentum operator, $\boldsymbol{\sigma}$ are Pauli matrices, and $\mathbf{c}$ is a unit vector normal to the layer. This term means violation of 2D in-plane parity, and, hence, one may expect that dynamics and kinetics of such systems will possess some new uncommon properties.

Recently some aspects of the electromagnetic wave frequency doubling by reflecting off such layers have been discussed in [3]. In papers [4, 5] an attempt has been made to interpret some features of magnetic-resistivity oscillations by means of Hamiltonian (1), though the successive theory of magneto-transport

The Hamiltonian of 2D motion without taking into account the interparticle interaction and impurity potential has the form

$$H = \frac{p^2}{2m} + \frac{\alpha}{\hbar}[\mathbf{pc}]\boldsymbol{\sigma}. \qquad (2)$$

For electron Green's function (solid lines in Figs. 1 and 2) we have the expression

$$G_{\alpha\beta}(\zeta, \mathbf{p}) = (\zeta - H)^{-1} = \frac{\Omega^{(+)}_{\alpha\beta}(\mathbf{p})}{\zeta - E_{(+)}(p)} + \frac{\Omega^{(-)}_{\alpha\beta}(\mathbf{p})}{\zeta - E_{(-)}(p)}, \qquad (3)$$

where

$$E_{(\pm)}(p) = \frac{p^2}{2m} \pm \frac{\alpha}{\hbar}p \qquad (4)$$

are the energies of two branches of the energy spectrum, corresponding to positive and negative eigenvalues of the spirality operator

$$\hat{\nu}(\mathbf{p}) = [\mathbf{pc}]\boldsymbol{\sigma}/p \qquad (5)$$

and

The IREE in Bi

The IREE[1,2] : Spin-conversion at the Bi/Ag(111) interface [3]

1) V. Edelstein, Solid State Comm. 73, 233 (1990).
2) J.-C. Rojas-Sanchez et al., Nature Comm. 4, 2944 (2013).
3) A large spin splitting (200 meV) C. Ast et al., PRL 2007.

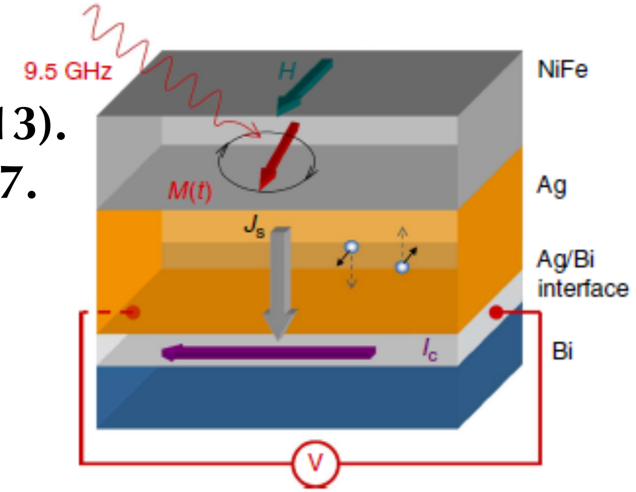

Conversion rate : the IREE length

$$\lambda_{IREE} = 0.3\ \mathrm{nm}$$

/ The electrons at the interface obey to the 2D Hamiltonian?
/ Spin current is 100% converted to charge current?
/ How does self-induced electromotive forces
from NiFe (Py) contribute to the IREE signals?

The self-induced ISHE from NiFe :
A. Tsukahara, M.S. et al., PRB 89, 235317 (2014).
PHE from NiFe :
L.Chen, H. Ohno et al., APEX 7, 013002 (2014).

Significant follow-up study

Applied Physics Express **9**, 033001 (2016)
http://doi.org/10.7567/APEX.9.033001

Experimental observation of spin-to-charge current conversion at non-magnetic metal/Bi_2O_3 interfaces

Shutaro Karube[1,2], Kouta Kondou[2], and YoshiChika Otani[1,2]

[1]Institute for Solid State Physics, University of Tokyo, Kashiwa, Chiba 277-8581, Japan
[2]Center for Emergent Matter Science, RIKEN, Wako, Saitama 351-0198, Japan

Received December 16, 2015; accepted January 6, 2016; published online January 27, 2016

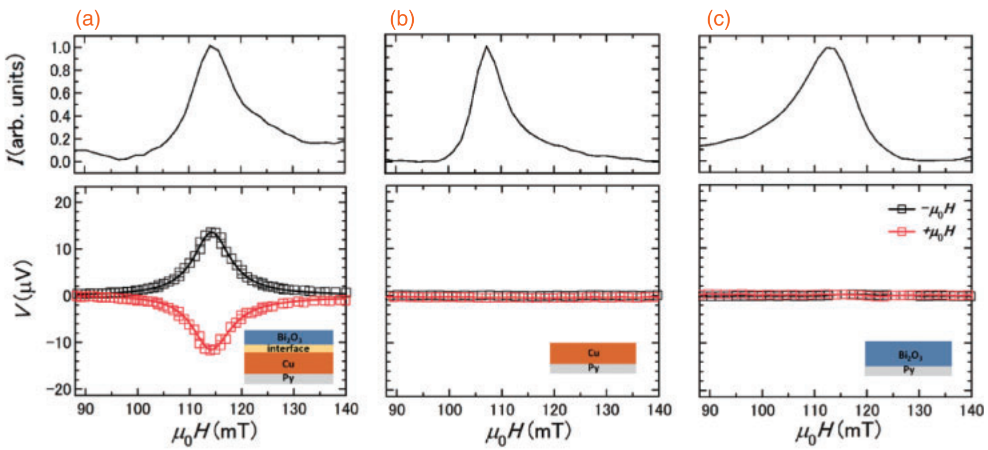

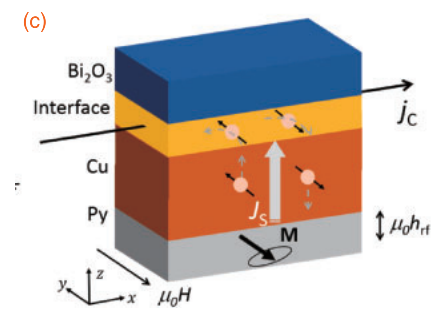

/ BiO, instead of Bi : Spin current is blocked.
/ Bi/Cu, instead of Bi/Ag
/ The IREE length : 0.6 nm (double)

Purpose of this study

Further investigation of a spin conversion mechanism
in poly-Bi & Bi/Ag on YIG, the ferrimagnetic insulator.
(no unwanted EMFs from spin source materials)

/ ISHE ? IREE ?
/ Multi-carrier effect ?

Experimental

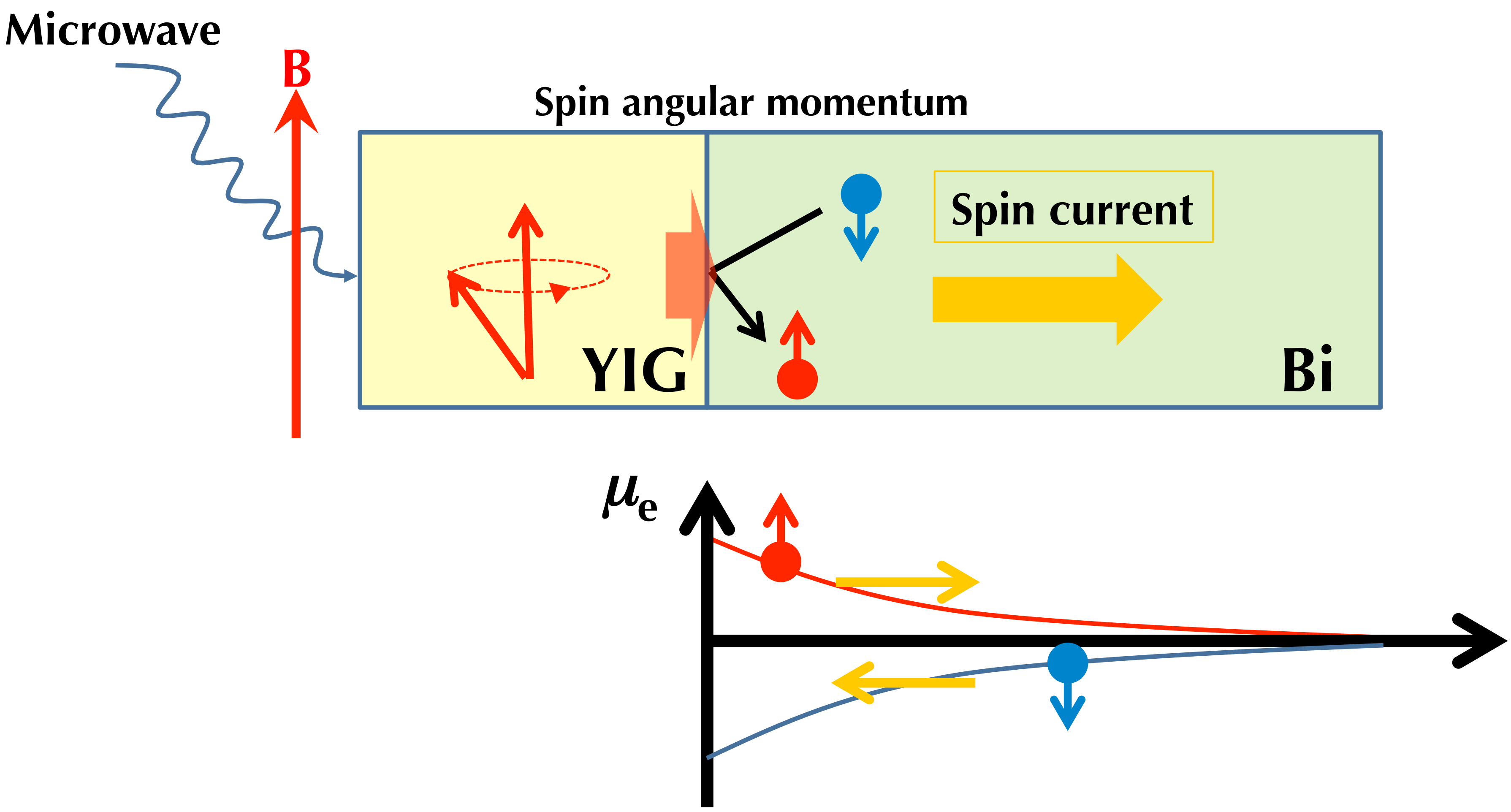

S. Mizukami, Y. Ando, and T. Miyazaki, PRB 66, 104413 (2002).
Y. Tserkovnyak and A. Brataas, PRL 88, 117601 (2002).

How to distinguish them?

ISHE

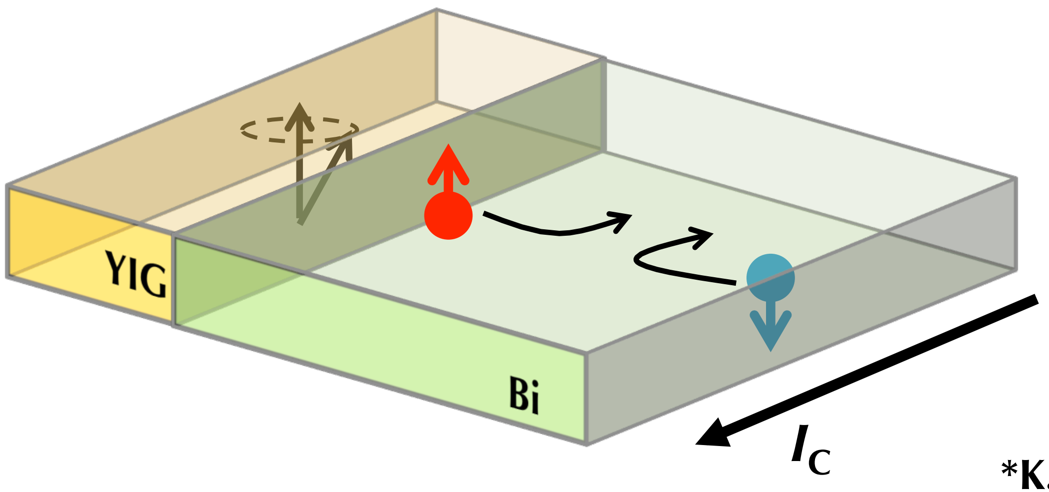

d_{Bi}: Bi thickness
λ_S: spin dif. length

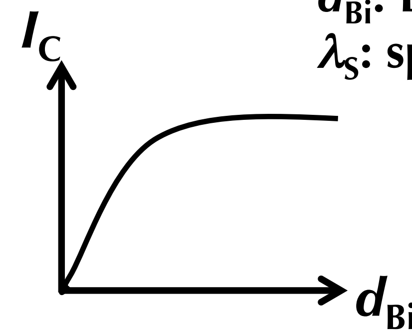

$$* \; I_C \propto \tanh\left(d_{Bi} \big/ 2\lambda_S \right)$$

*K. Ando et al., JAP 108, 113925 (2010).

IREE

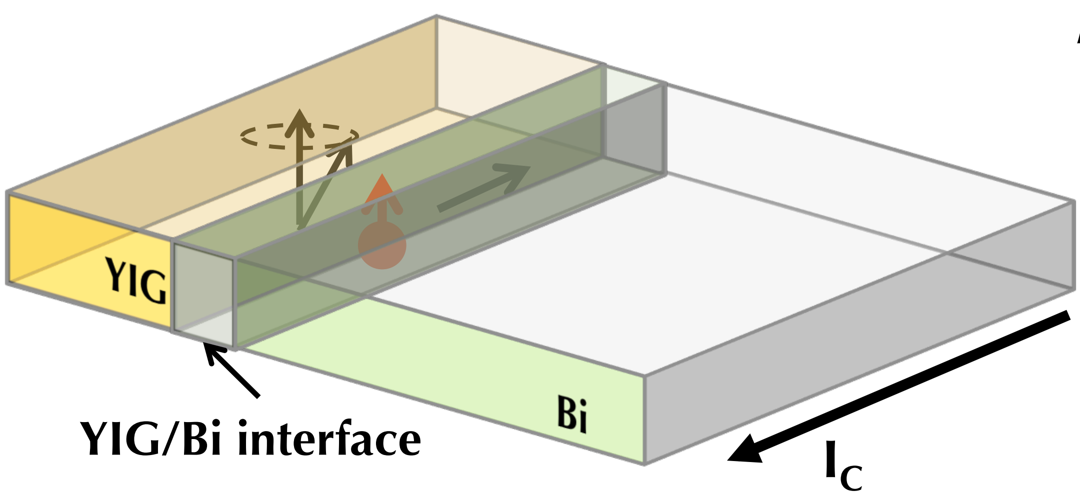

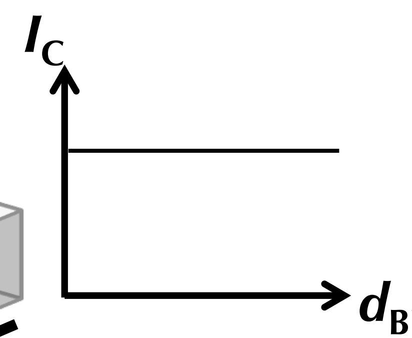

I_C should be constant !!

Sample preparation

Structure

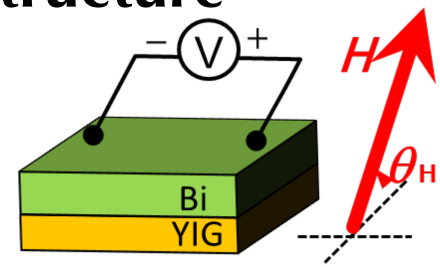

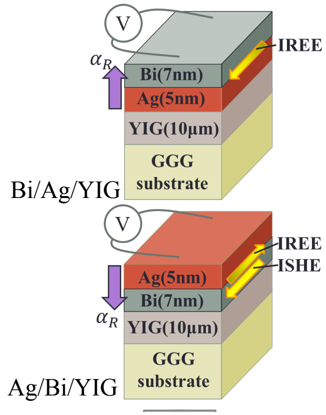

- Single crystal YIG
- Bi: thermal evaporation ($P_{base}=10^{-7}$ Pa)

Poly-Bi, Bi/Ag & Ag/Bi on YIG

X-ray diffraction

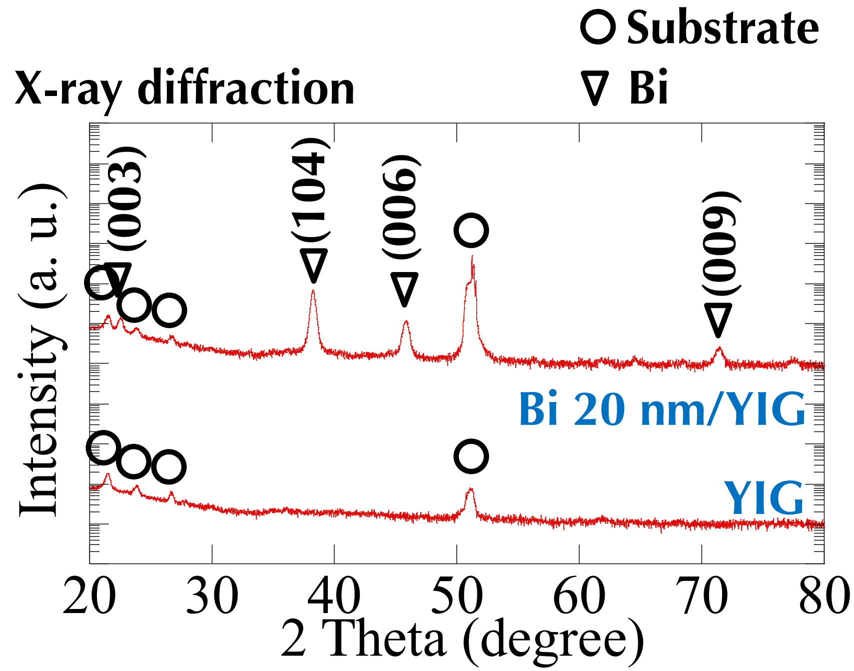

Measurement

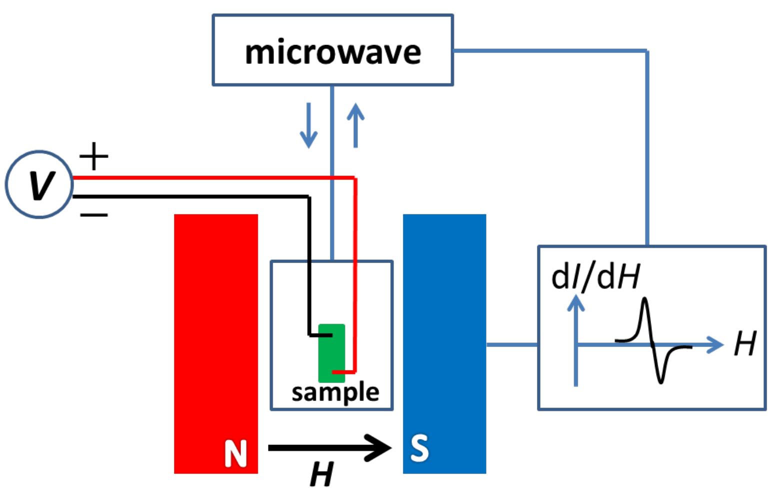

1. ESR (made by JEOL)
   Cavity : TE_{011}
   Frequency : 9.12 GHz
   Temperature: RT
2. Hall measurement
   d=8~70 nm, T=2~300 K
3. Magnetoresistance
   B= ±5 T

Hall measurement & magnetoresistance (MR)

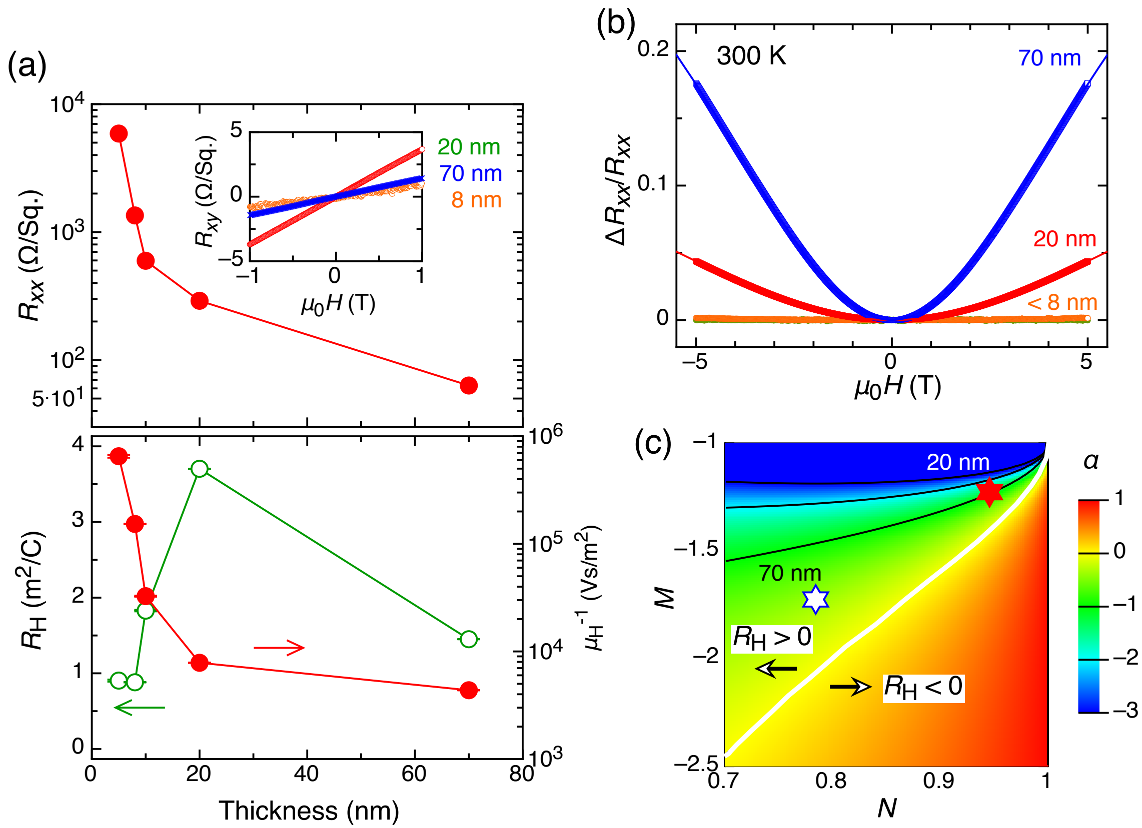

Two carrier analysis of Hall measurements

See also,
G. Eguchi et al.,
Phys. Rev. B91, 235117 (2015).

R_H : Sheet Hall resistivity

$$R_H = R_0 \cdot \alpha = R_0 \frac{2M + N + NM^2}{(N+M)^2}$$

$$R_0 = [(n_1 + n_2)q_1]^{-1}$$

$R_H > 0$, $\alpha < 0$: electron

MR :

$$\frac{R_{xx}(B) - R_{xx}(0)}{R_{xx}(B)} = \frac{(N^2-1)M^2(1-M^2)\mu_H^2B^2}{(2M+N+NM^2)^2 + (N^2-M^2)(1-M^2)\mu_H^2B^2}$$

$$N = (n_1 - n_2)/(n_1 + n_2) \qquad M = (\mu_1 - \mu_2)/(\mu_1 + \mu_2)$$

$$\mu_H = \frac{\mu_1 + \mu_2}{2} \cdot \beta = \frac{\mu_1 + \mu_2}{2} \cdot \frac{2M + N + NM^2}{N+M}$$

n : carrier ($n_1 > n_2$)
m : mobility

Central result in the Hall measurements of Bi

/ For 20 nm Bi

$N= 0.96$, $M= -1.12$, $\mu_H=0.0127\ m^2/Vs$

Electron is the majority carrier.

$n_1=1.76e18\ /m^2$, $n_2=0.04e18\ /m^2$

$\mu_1=0.0099\ m^2/Vs$, $\mu_2=0.11\ m^2/Vs$

Hole mobility is greater.

/ For 70 nm Bi

$N= 0.78$, $M= -1.72$, $\mu_H=0.0230\ m^2/Vs$

Electron is the majority carrier.

$n_1=1.43e18\ /m^2$, $n_2=0.18e18\ /m^2$

$\mu_1=0.047\ m^2/Vs$, $\mu_2=0.18\ m^2/Vs$

Hole mobility is greater.

Electromotive forces from Bi

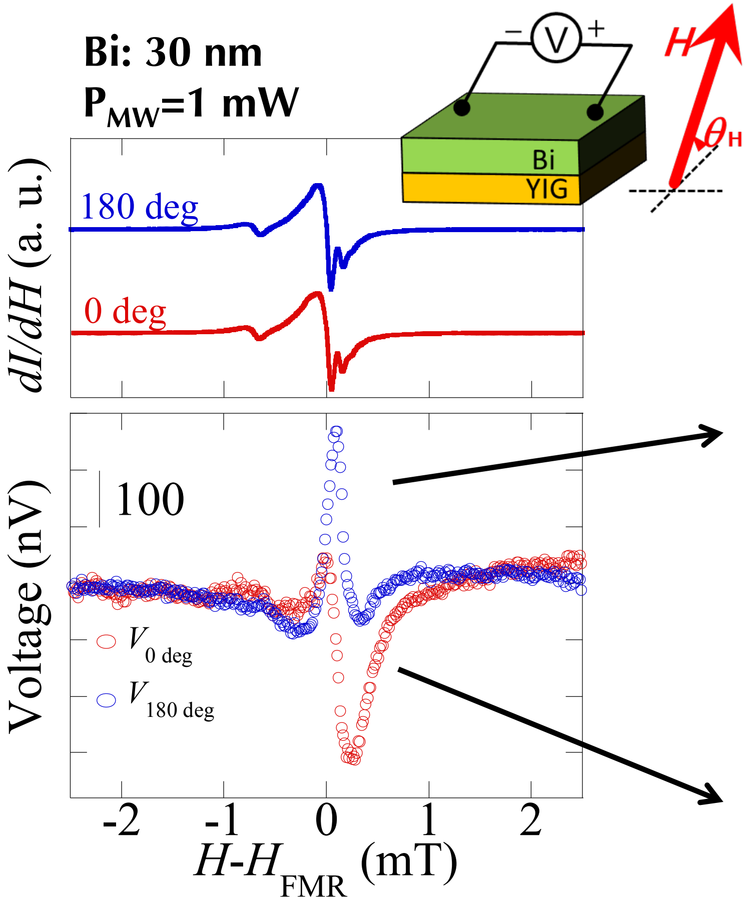

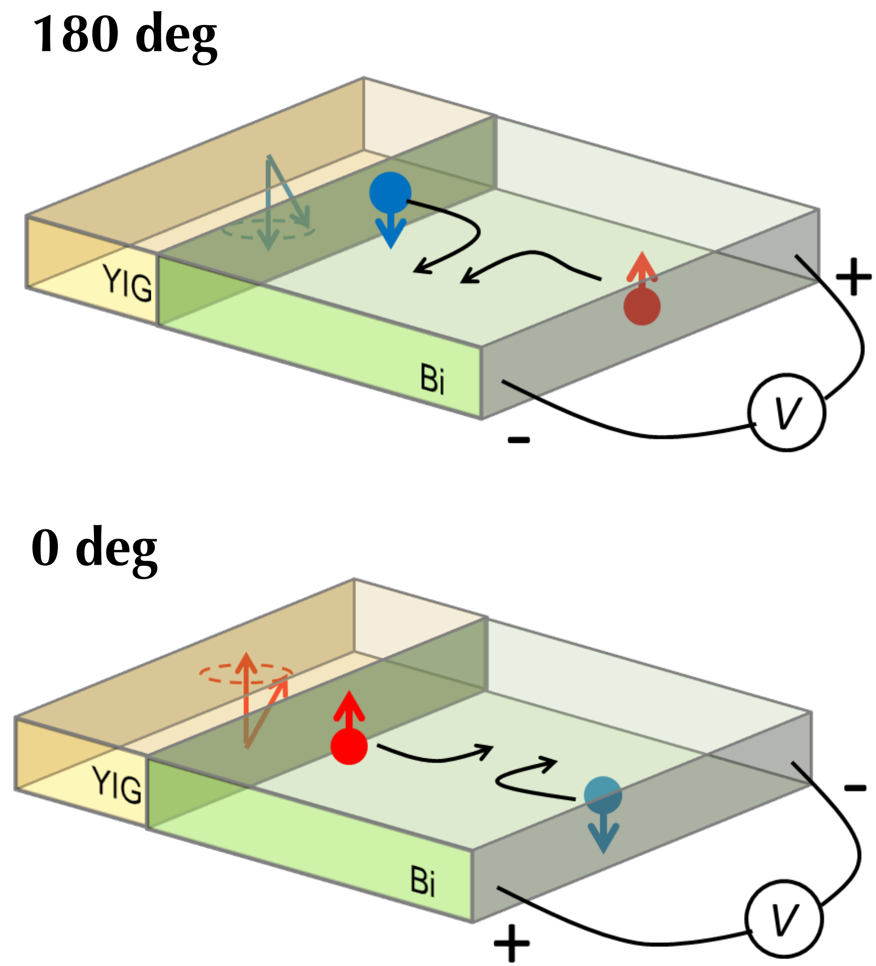

* $\mathbf{j}_C \propto \mathbf{j}_S \times \boldsymbol{\sigma}$

j_C : charge current

j_S : spin current

σ: spin polarized vector

*E. Saitoh et al., APL 88, 629 (2006).

Thickness dependence of EMFs from Bi

Thickness dependence of a generated electric current, $I_C = V_{ISHE}/R$

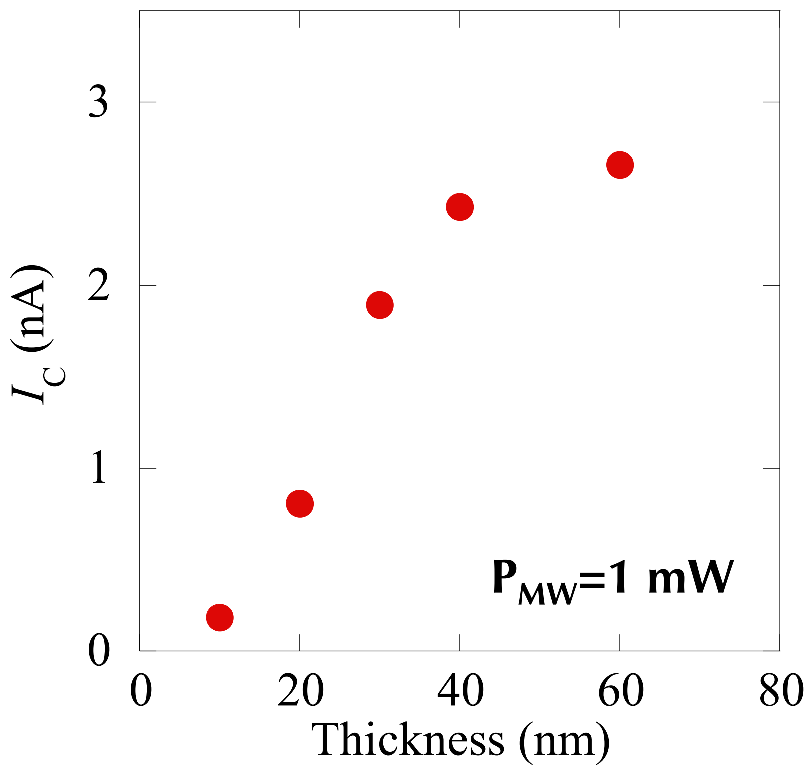

ISHE

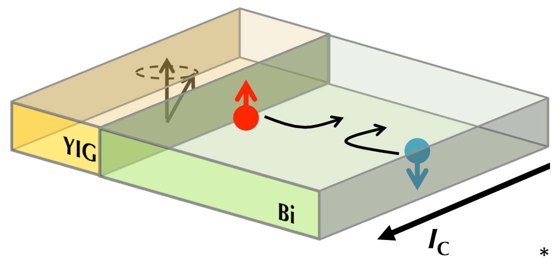

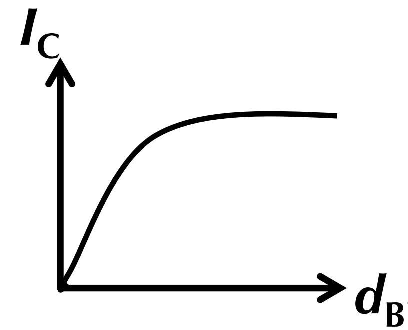

$$^{*}\, I_C \propto \tanh\left(d_{Bi} / 2\lambda_S \right)$$

*K. Ando et al., JAP 108, 113925 (2010).

IREE

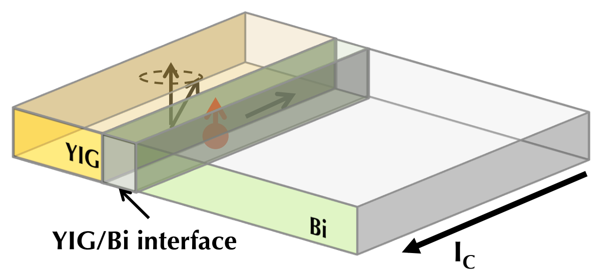

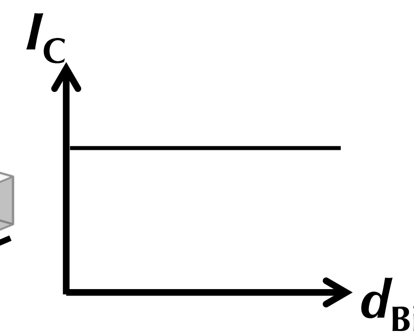

Thickness dependence of EMFs from Bi

Thickness dependence of a generated electric current, $I_C = V_{ISHE}/R$

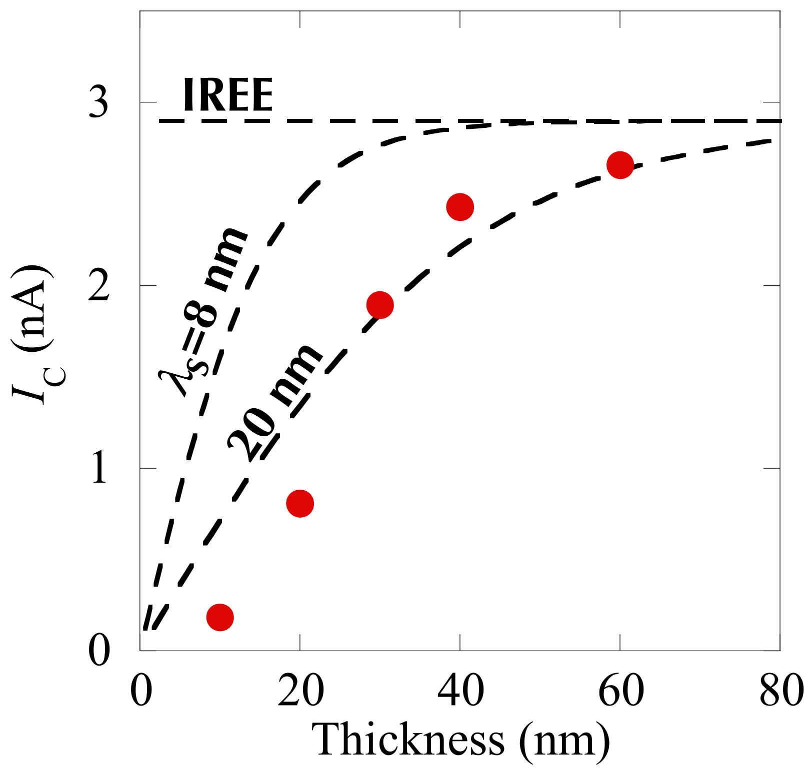

ISHE

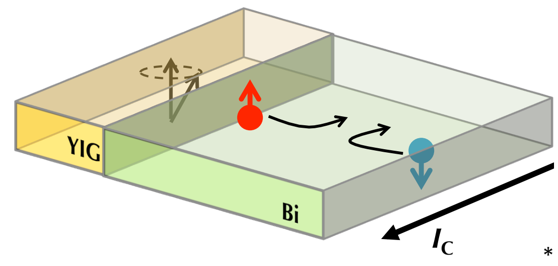

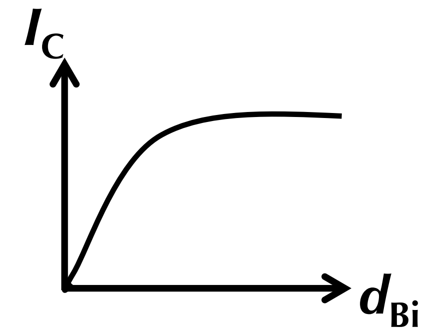

$$^{*} I_C \propto \tanh\left(\frac{d_{Bi}}{2\lambda_S}\right)$$

*K. Ando et al., JAP 108, 113925 (2010).

IREE

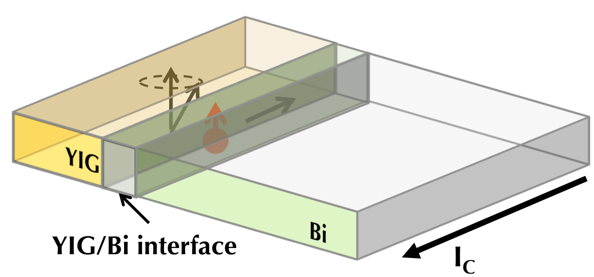

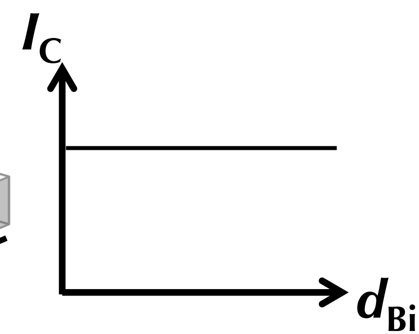

No IREE in Bi/YIG !!

Topological Insulator

BiSbTeSe (3D, n-type)

Yuichiro Ando, M.S. et al., Nano Lett. 2014.

TlBiSe (3D, p-type)

G. Eguchi, M.S. et al., PRB(R) 2014.

Ibid., PRB 2015.

Hall effect, Quantum Hall effect and more

Hall effect

External magnetic field : B_z

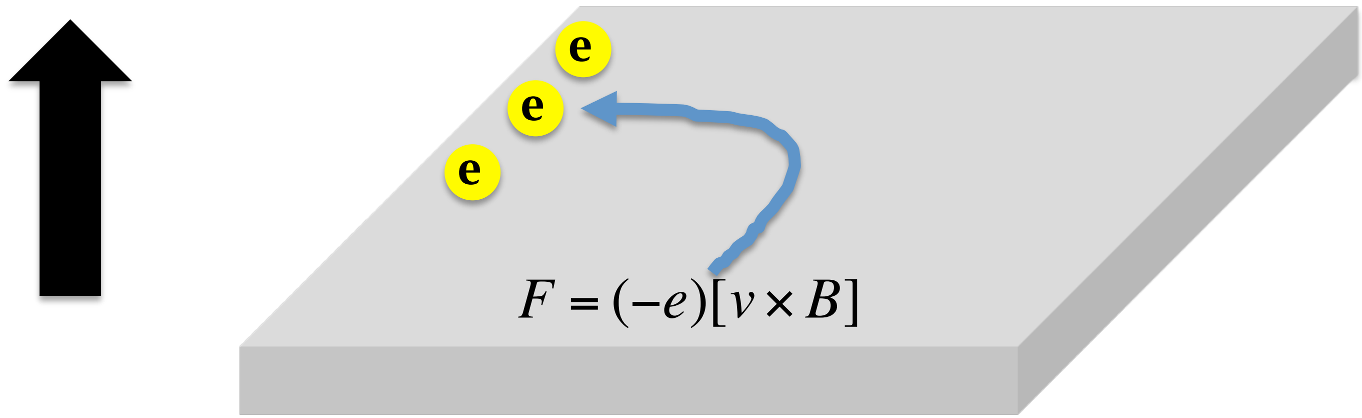

Hall conductivity

$$J_x = \sigma_{xy} E_y$$

/ Time reversal symmetry breaking (J : odd, E: even)
/ Parity symmetry breaking (in 2-D, J_x & J_y, opposite parity)
/ $J \perp E$, no energy dissipation

External magnetic field breaks P & T symmetry in the Hall effect.

Hall effect, Quantum Hall effect and more

Quantum Hall effect

2-D system with non-zero energy gap

External magnetic field : B_z

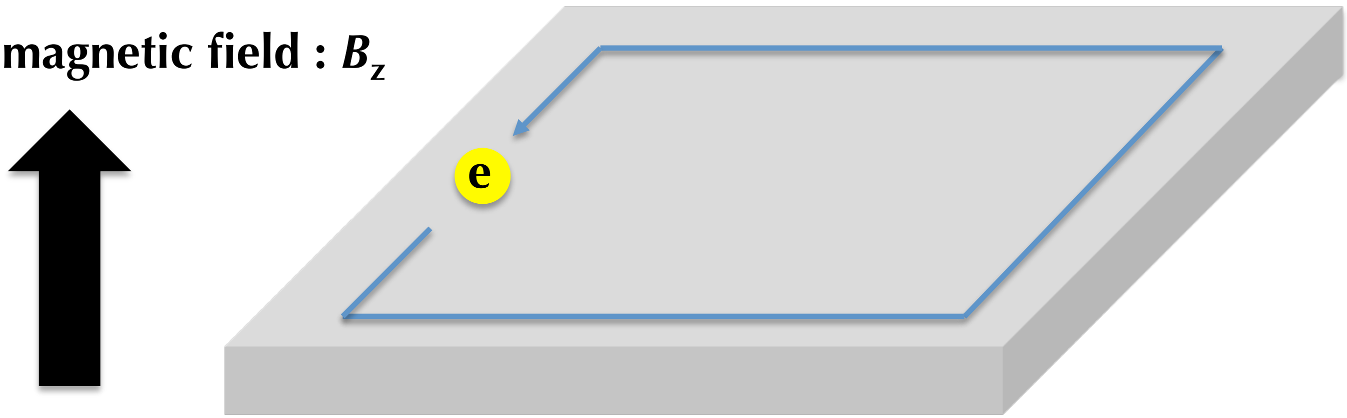

External magnetic field breaks time reversal symmetry.

Quantum Hall conductivity (derived by Kubo formula)

$$\sigma_{xy} = \frac{e^2}{2\pi} \sum_{n \le E_F} \int_{BZ} \frac{d^2k}{2\pi i} \left(\left\langle \frac{\partial u^n_{k(t)}}{\partial k_x} \middle| \frac{\partial u^n_{k(t)}}{\partial k_y} \right\rangle - \left\langle \frac{\partial u^n_{k(t)}}{\partial k_y} \middle| \frac{\partial u^n_{k(t)}}{\partial k_x} \right\rangle \right)$$

$$= \frac{e^2}{2\pi} N_{ch}$$

Chern #(topological #): integer
[# of geometrically singular points]
⇒ Berry phase !

Time-dependent Schrödinger Eq. for Bloch states

$$i \left| \dot{u}^n_{k(t)} \right\rangle = H_{k(t)} \left| u^n_{k(t)} \right\rangle$$

Quantum spin Hall effect

Spin Hall conductivity & spin Chern # :

$$\sigma_{xy}^{\uparrow}=\frac{e^2}{2\pi}\sum_{n\le E_F}\int_{BZ}\frac{d^2k}{2\pi i}\left(\left\langle\frac{\partial u_{k(t)}^{\uparrow n}}{\partial k_x}\middle|\frac{\partial u_{k(t)}^{\uparrow n}}{\partial k_y}\right\rangle-\left\langle\frac{\partial u_{k(t)}^{\uparrow n}}{\partial k_y}\middle|\frac{\partial u_{k(t)}^{\uparrow n}}{\partial k_x}\right\rangle\right)=\frac{e^2}{2\pi}N_{ch}^{\uparrow}$$

$$\sigma_{xy}^{\downarrow}=\frac{e^2}{2\pi}\sum_{n\le E_F}\int_{BZ}\frac{d^2k}{2\pi i}\left(\left\langle\frac{\partial u_{k(t)}^{\downarrow n}}{\partial k_x}\middle|\frac{\partial u_{k(t)}^{\downarrow n}}{\partial k_y}\right\rangle-\left\langle\frac{\partial u_{k(t)}^{\downarrow n}}{\partial k_y}\middle|\frac{\partial u_{k(t)}^{\downarrow n}}{\partial k_x}\right\rangle\right)=\frac{e^2}{2\pi}N_{ch}^{\downarrow}$$

Spin current :

$$\left\langle J_{kx}^{s}\right\rangle=\frac{1}{2e}\left(\left\langle J_{kx}^{\uparrow}\right\rangle-\left\langle J_{kx}^{\downarrow}\right\rangle\right)=\sigma_{xy}^{s}E_y \qquad \sigma_{xy}^{s}=\frac{1}{2e}(\sigma_{xy}^{\uparrow}-\sigma_{xy}^{\downarrow})=\frac{e}{2\pi}N_{ch}^{s}$$

Spin Chern # : $N_{ch}^{s}=\frac{1}{2}(N_{ch}^{\uparrow}-N_{ch}^{\downarrow})$

If time reversal symmetry exists,

the spin Chern # is always integer and non-zero.

"more", quantum spin Hall effect : topological insulator

Nano spin conversion

Time reversal symmetry in quantum spin Hall system

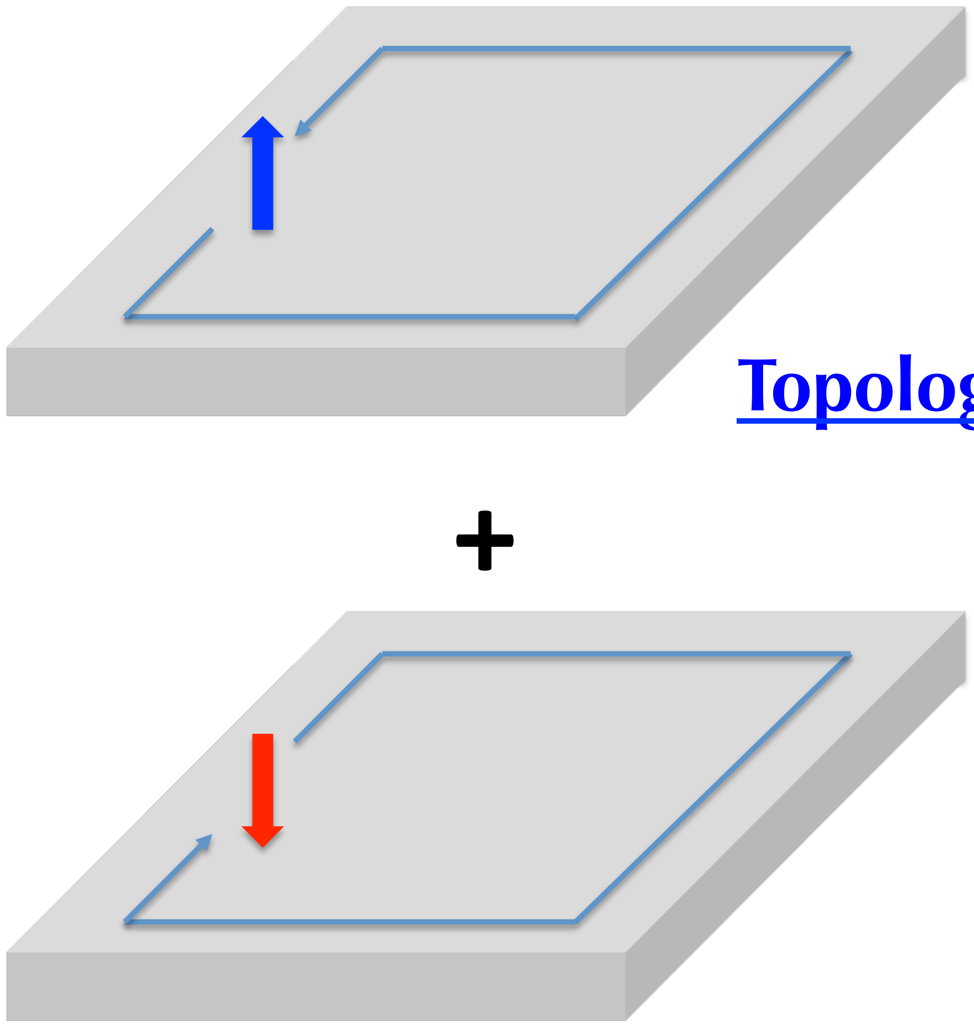

Topological Insulator !!

Non-zero Berry phase
always appears.
/ translational symmetry
/ wave number, k

⇒ Interface & edge
induce its discontinuity.
(Topological edge current)

Spin-momentum locking in topological insulator (TI)

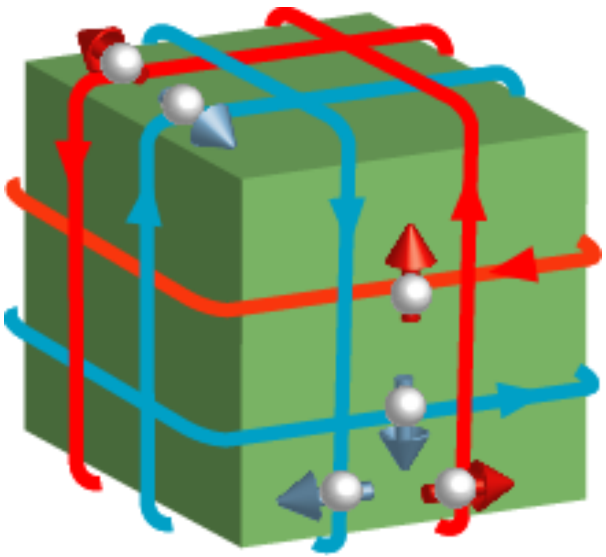

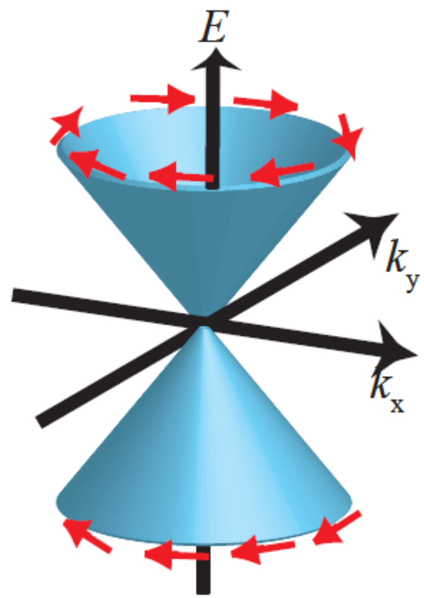

Dissipationless pure spin currents exist under thermal equilibrium.

TI : a new class of material

✓ 2D metallic surface state
✓ Dirac electron system
✓ Spin-momentum locking

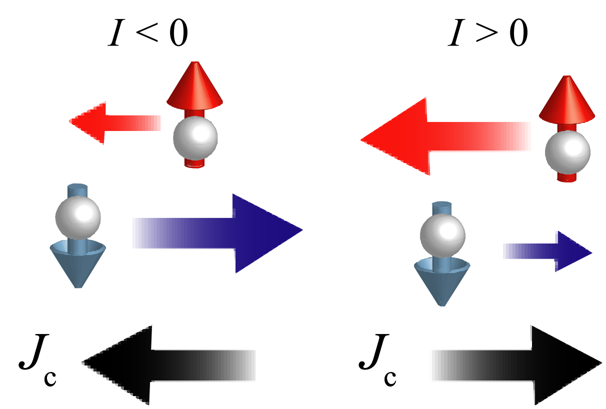

Objective

Electrical injection/extraction of the spin polarized current due to charge flow in the surface state of the topological insulator

Detection of the Dirac edge state

Nano spin conversion

Quantum Spin Hall Insulator State in HgTe Quantum Wells

Science, 318, 766 (2007).

Markus König,[1] Steffen Wiedmann,[1] Christoph Brüne,[1] Andreas Roth,[1] Hartmut Buhmann,[1] Laurens W. Molenkamp,[1]* Xiao-Liang Qi,[2] Shou-Cheng Zhang[2]

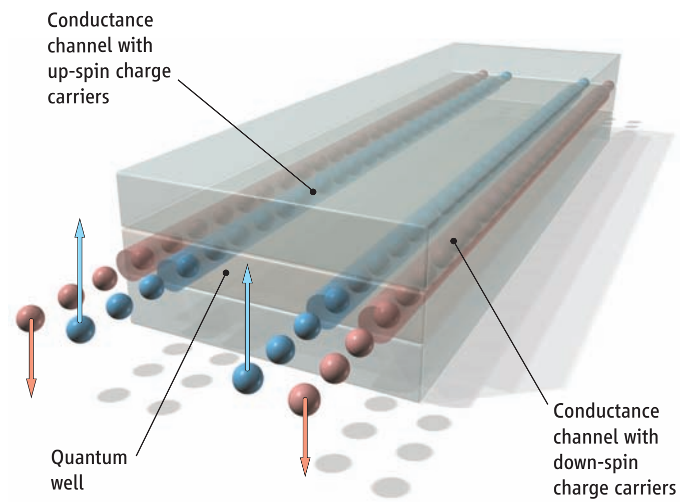

Schematic of the spin-polarized edge channels in a quantum spin Hall insulator.

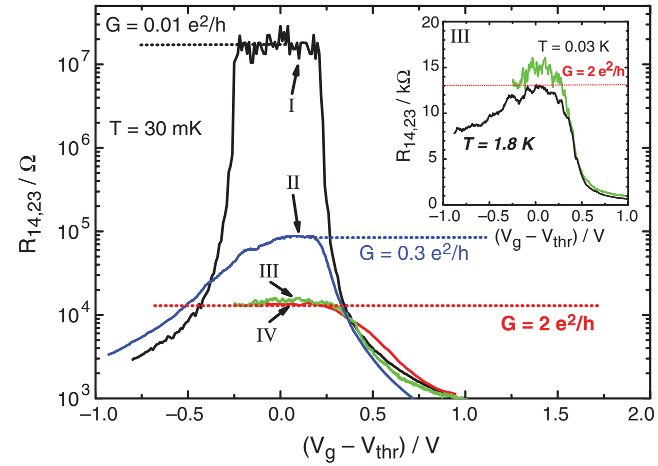

The first success of the electrical detection of the Dirac edge state.

(2-dimensional topological insulators, HgTe)

A challenge to detect the Dirac edge state in 3D TI

nature nanotechnology | ARTICLES
PUBLISHED ONLINE: 23 FEBRUARY 2014 | DOI: 10.1038/NNANO.2014.16

Electrical detection of charge-current-induced spin polarization due to spin-momentum locking in Bi_2Se_3

C. H. Li[1]*, O. M. J. van 't Erve[1], J. T. Robinson[2], Y. Liu[3], L. Li[3] and B. T. Jonker[1]*

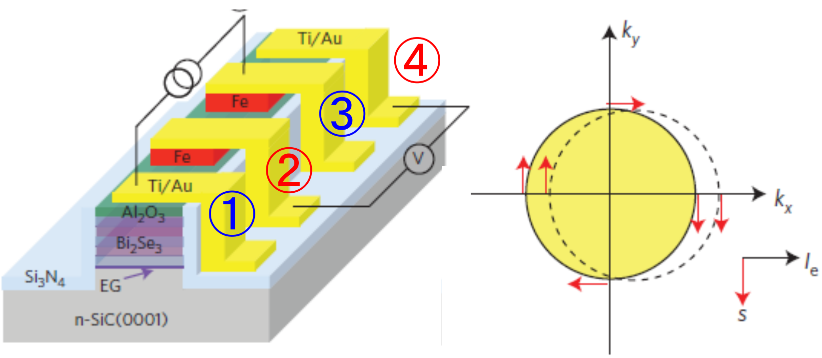

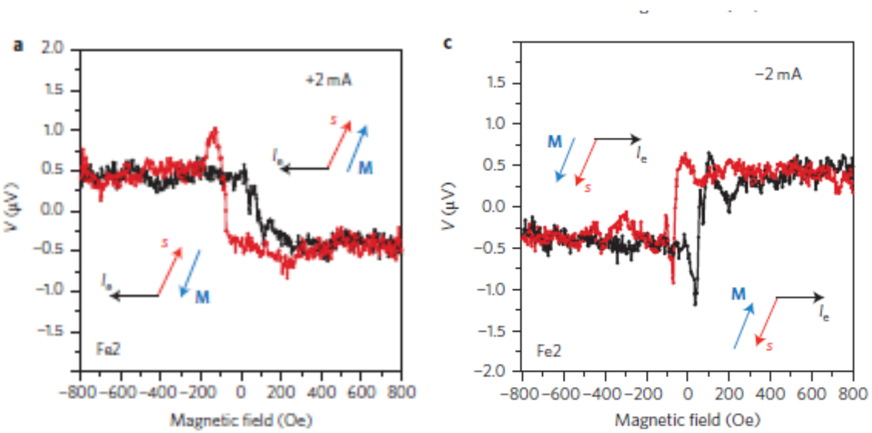

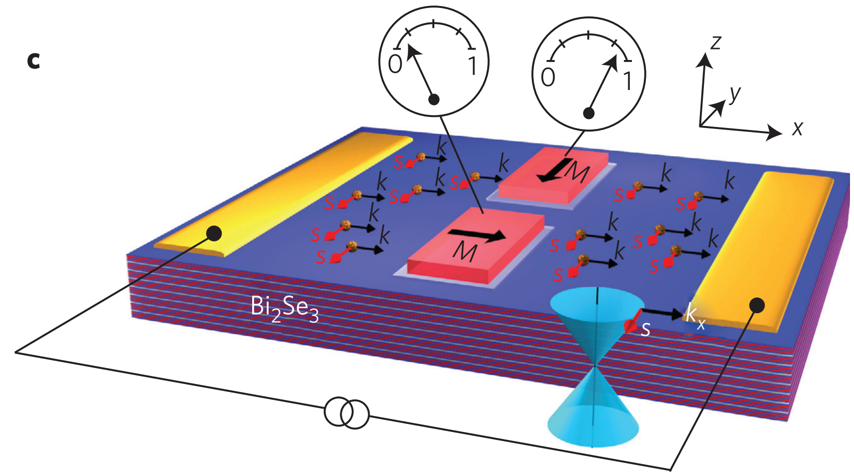

Our strategy

✓ Bulk-insulating TI
✓ Extraction of spin current by electric fields.
(Local magnetoresistance)

Our detection method of spin-momentum

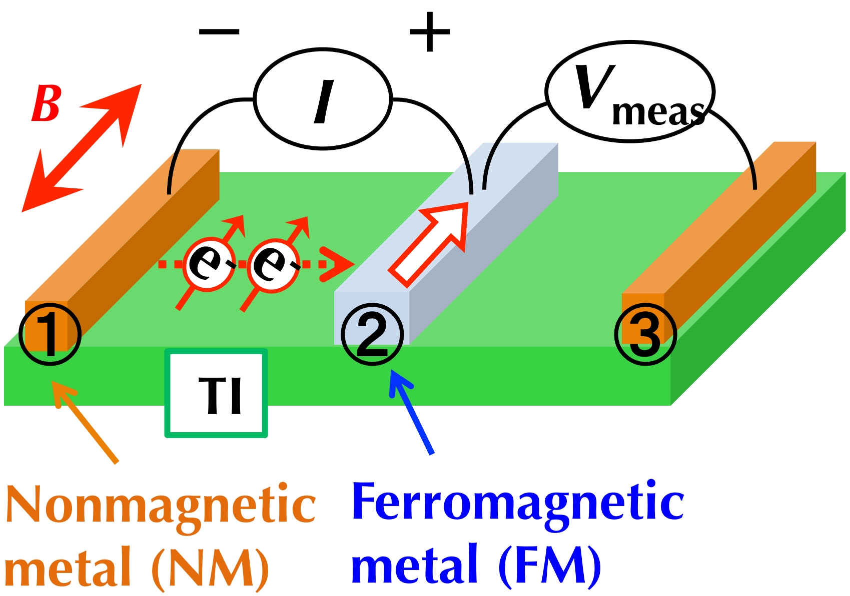

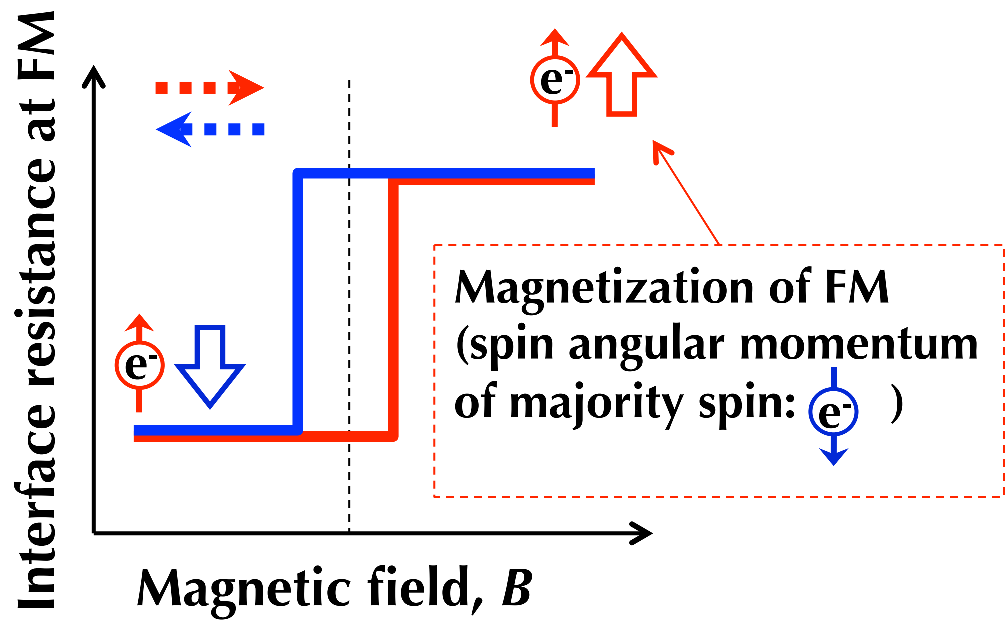

Our detection method of spin-momentum locking

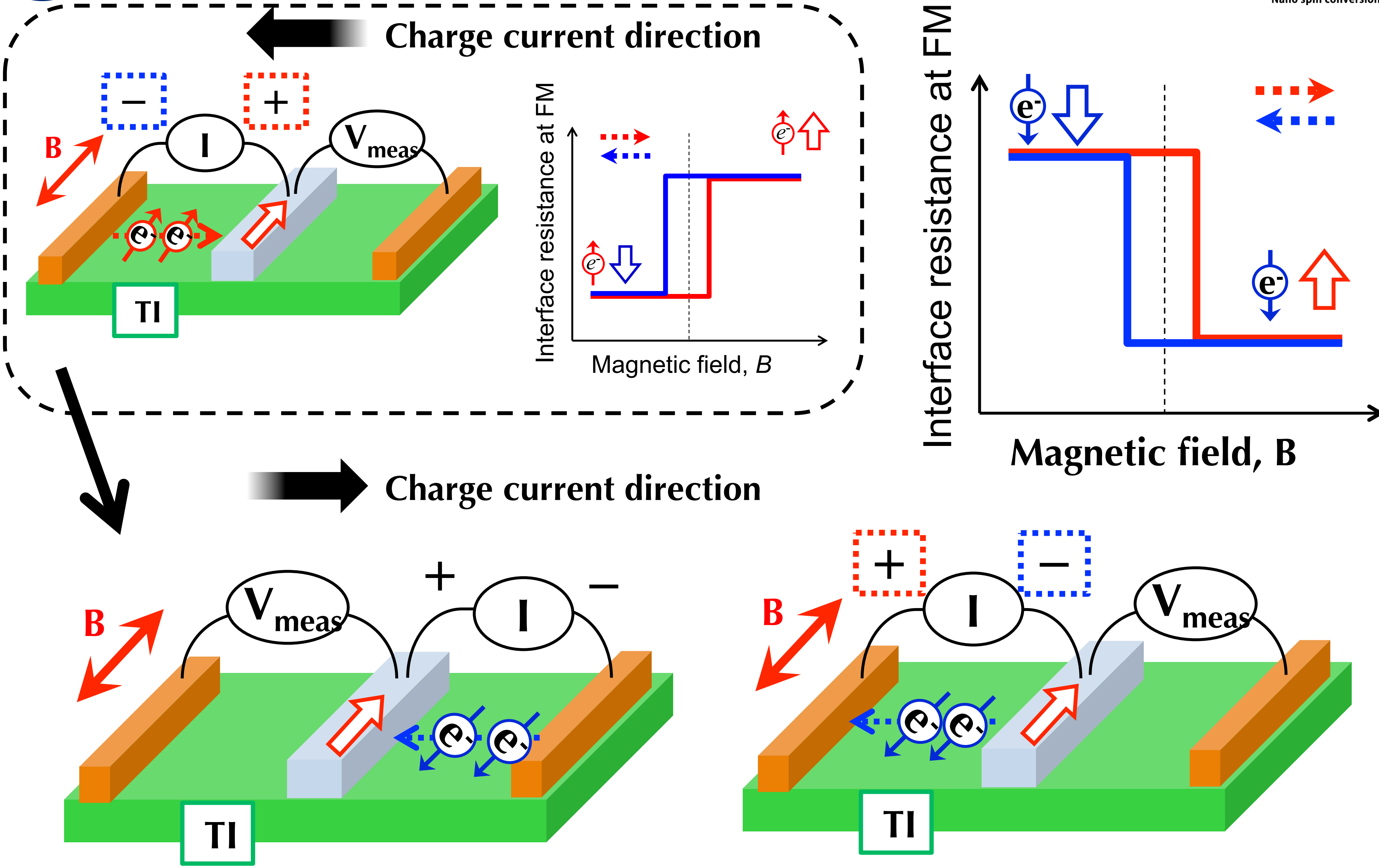

Change of current-voltage configuration

Change of current direction

Device fabrication procedure

Sample : Single crystal $Bi_{1.5}Sb_{0.5}Te_{1.7}Se_{1.3}$ (BSTS) formed by a Bridgeman method

Substrate : Thermally-oxidized SiO_2 (500 nm) / Si

TI flakes : Mechanical exfoliation using a Scotch tape

Measurement of TI-flake thickness: Laser microscope & Atomic force microscope.

$Ni_{80}Fe_{20}$(Py) & Au/Cr electrode : Electron beam lithography & Electron beam evaporation.

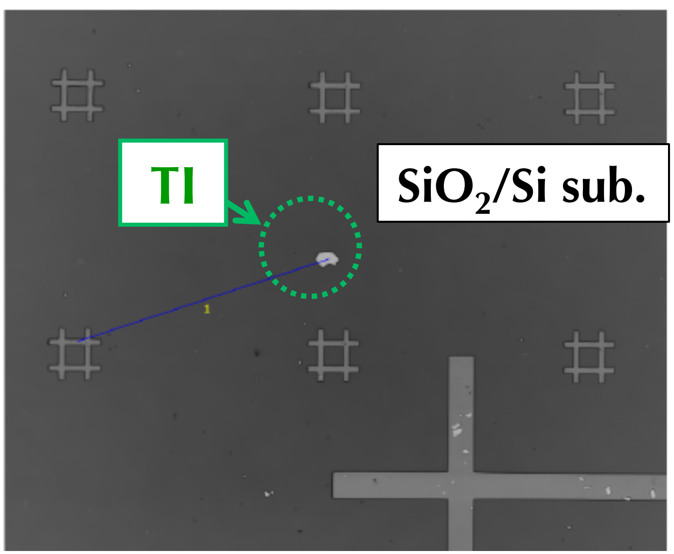

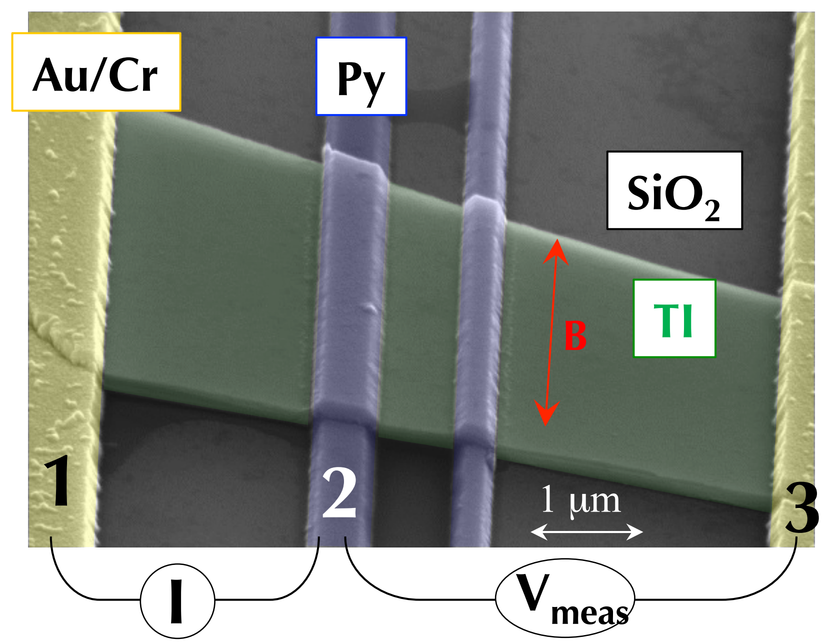

Temperature dependence of resistivity

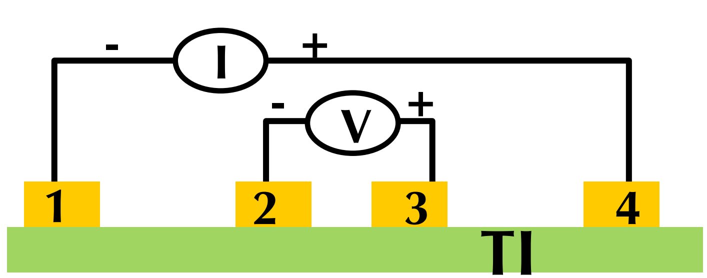

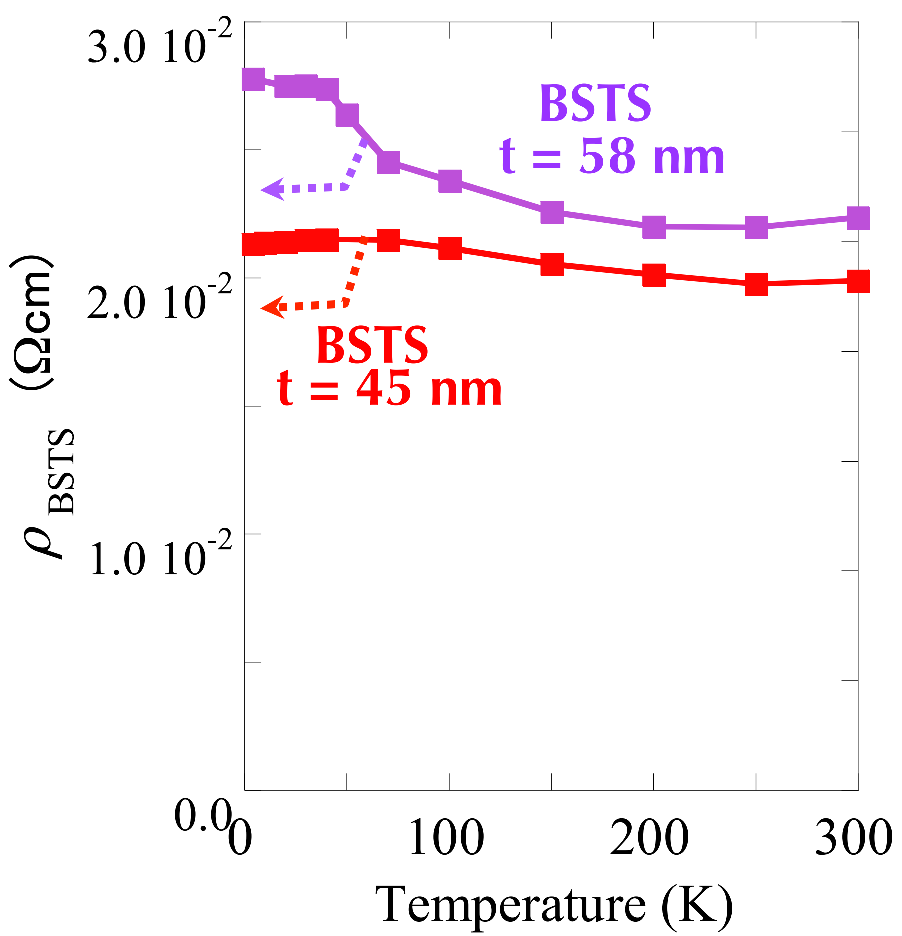

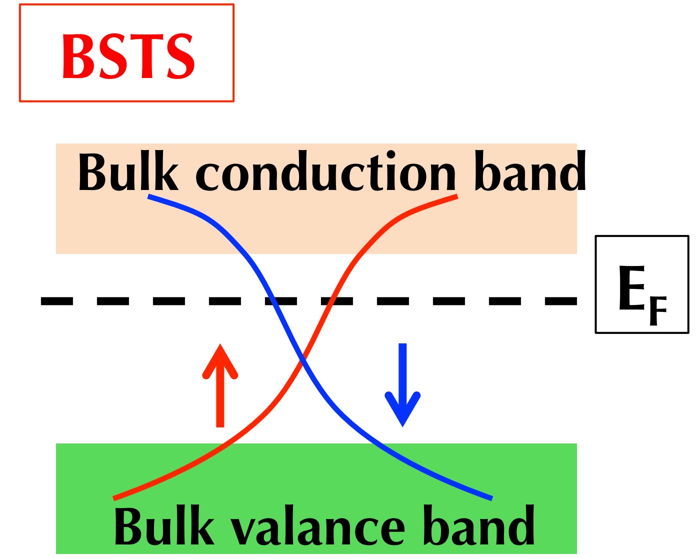

Temperature dependence of resistivity

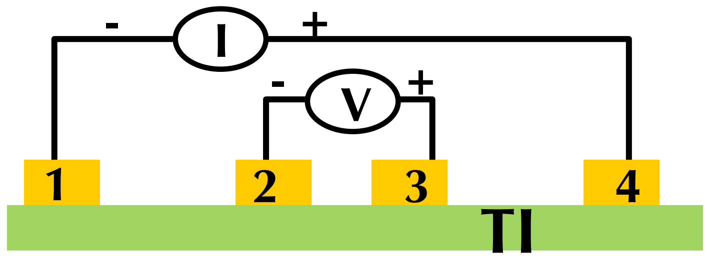

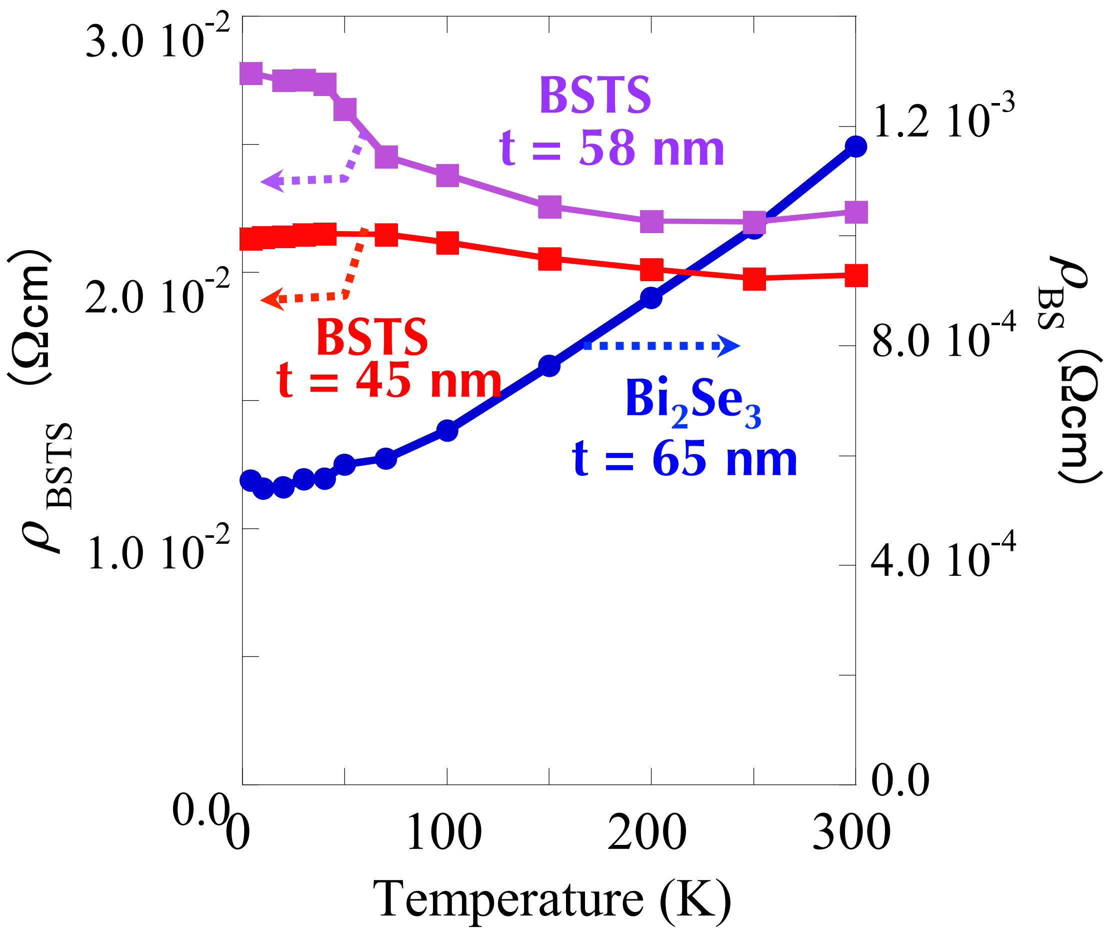

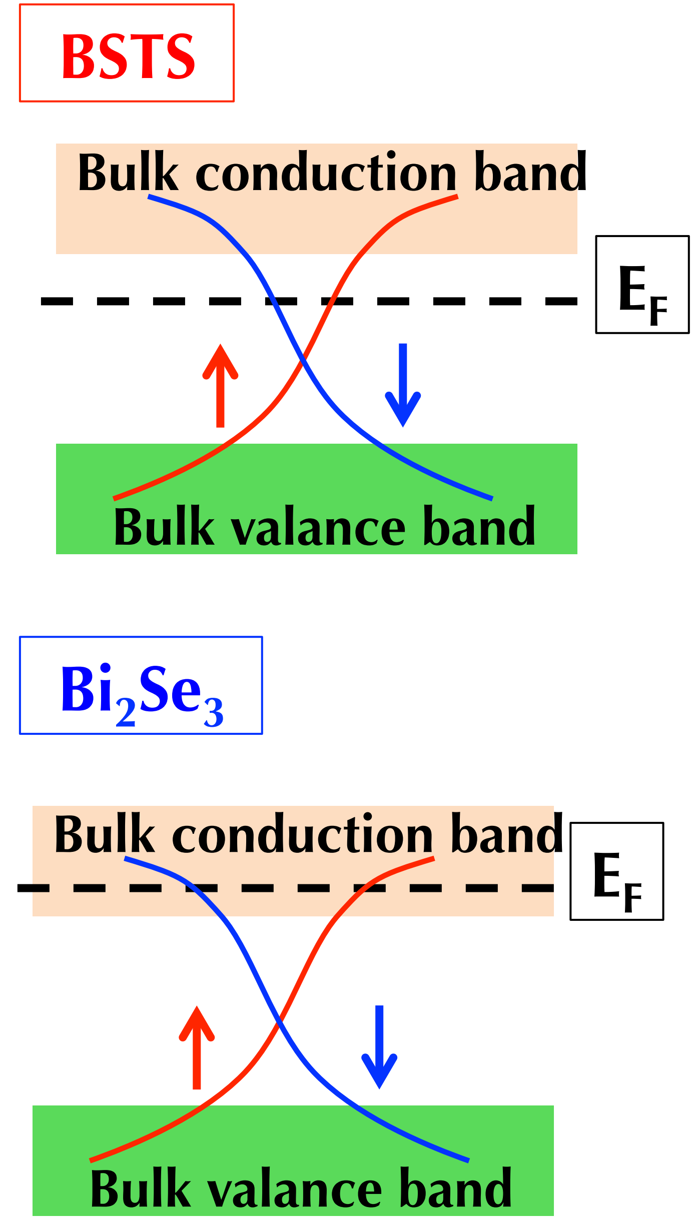

Magnetoresistance from the BSTS device

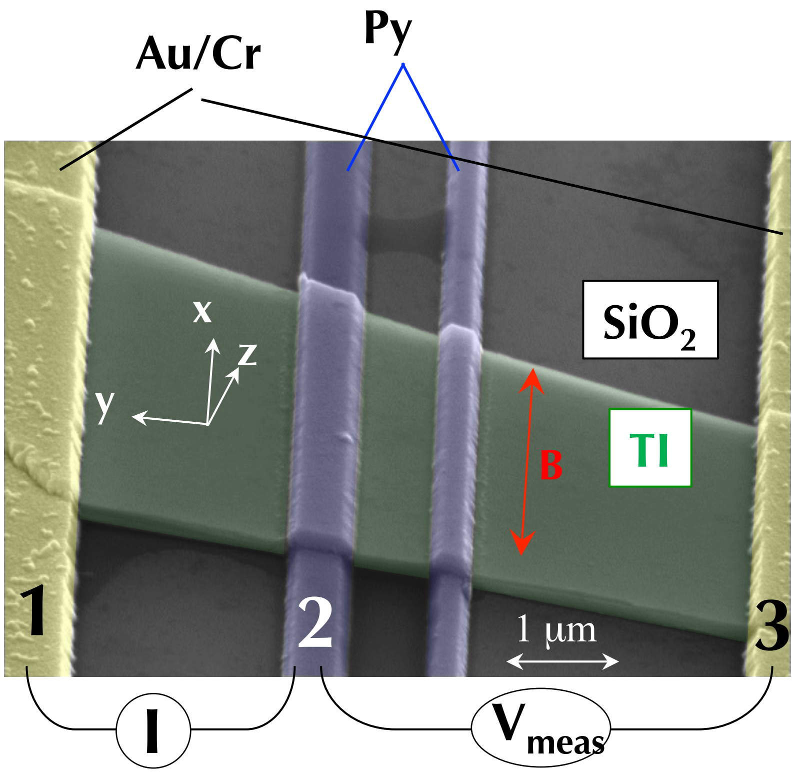

Applied current, I =100 μA

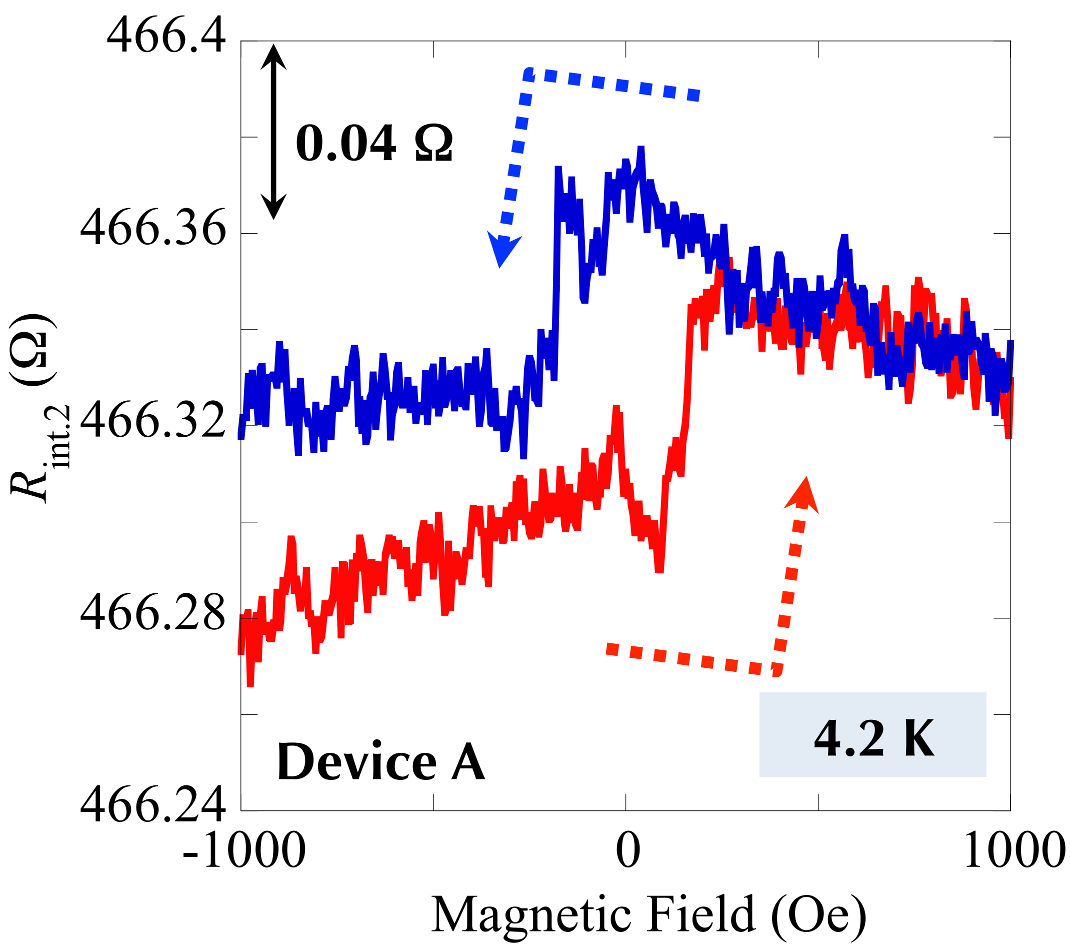

A hysteresis signal is observed.

Magnetoresistance from the BSTS device

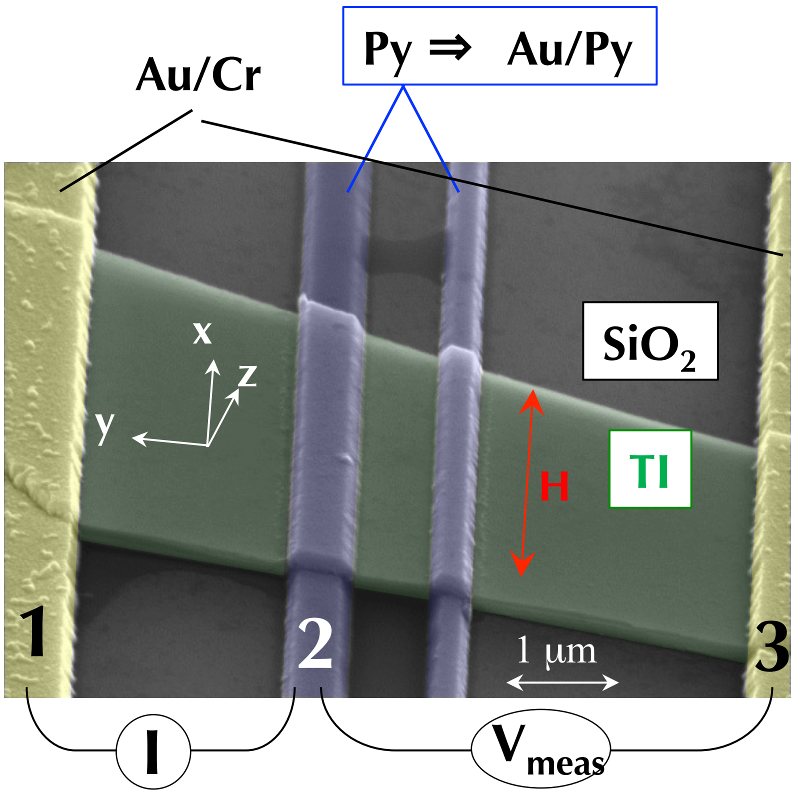

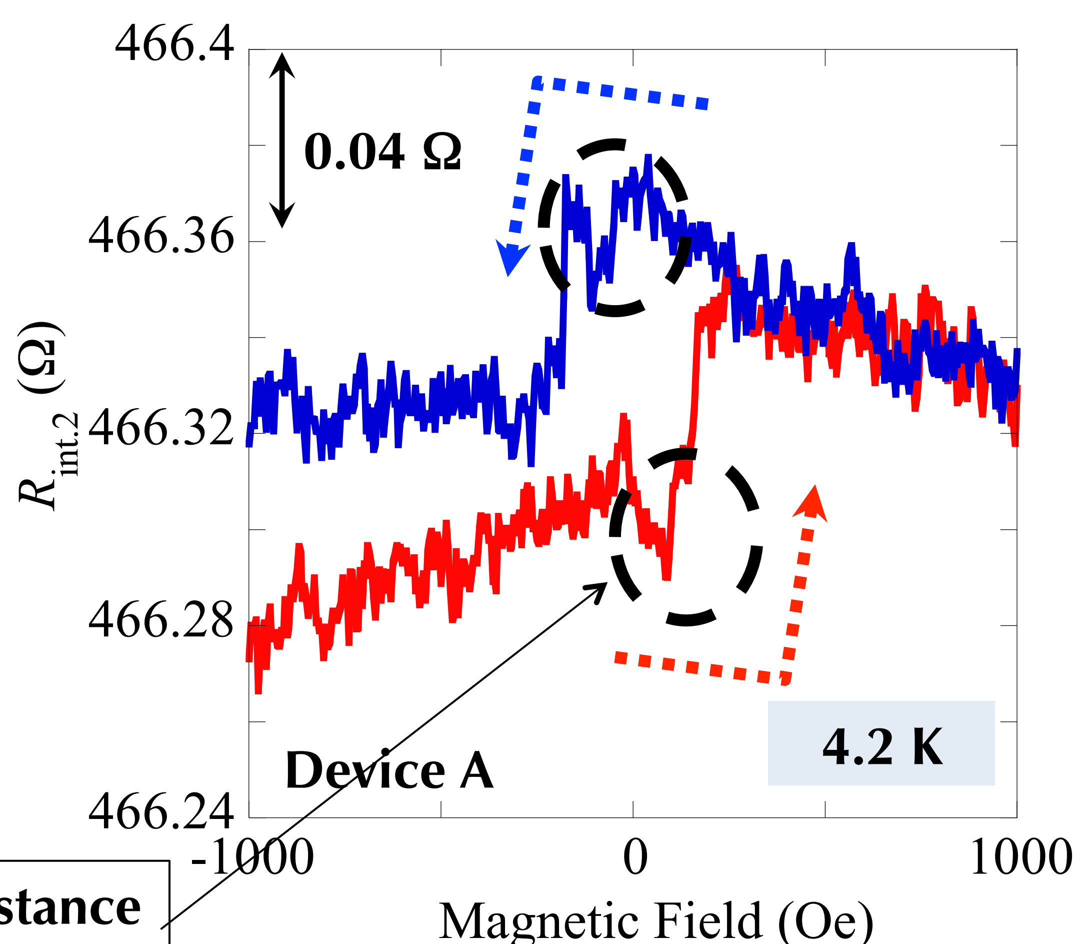

Anisotropic magnetoresistance (AMR)

A hysteresis signal is observed.

Polarity of the magnetoresistance

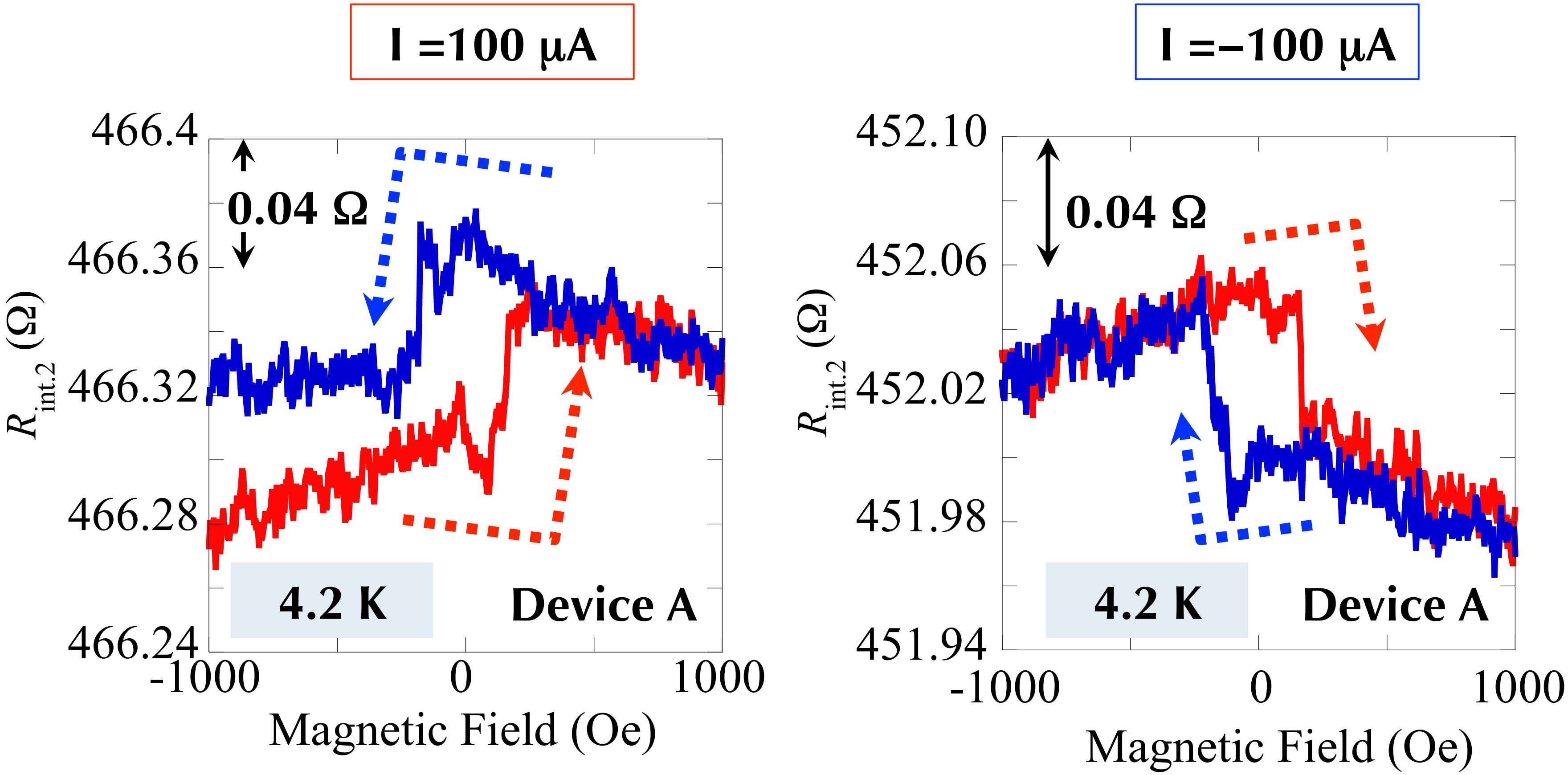

The polarity of the rectangular hysteresis signal reverses when the polarity of I is reversed.

Temperature dependence of MR from the BSTS

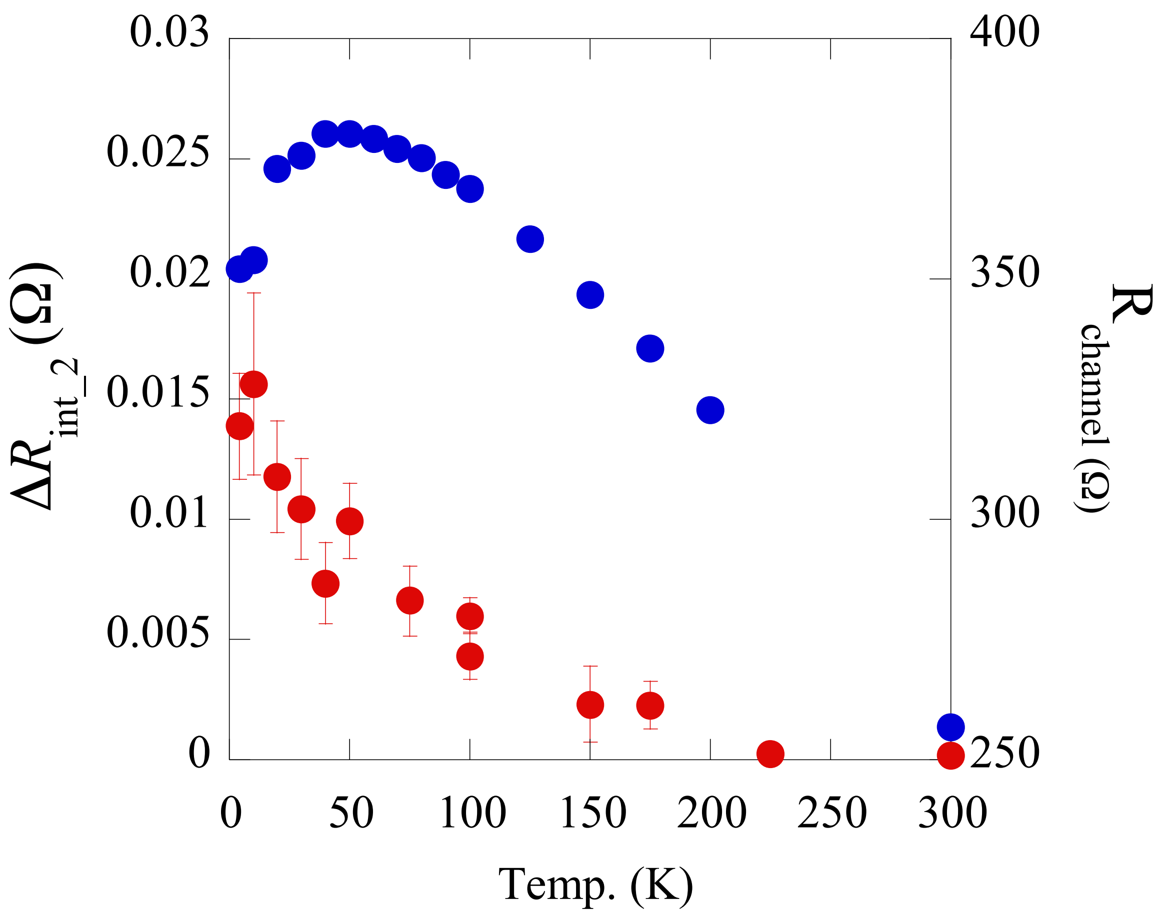

Disappearance of the rectangular signals : 150~200 K

Magnetoresistance from BiSe (not bulk insulative)

I =100 mA

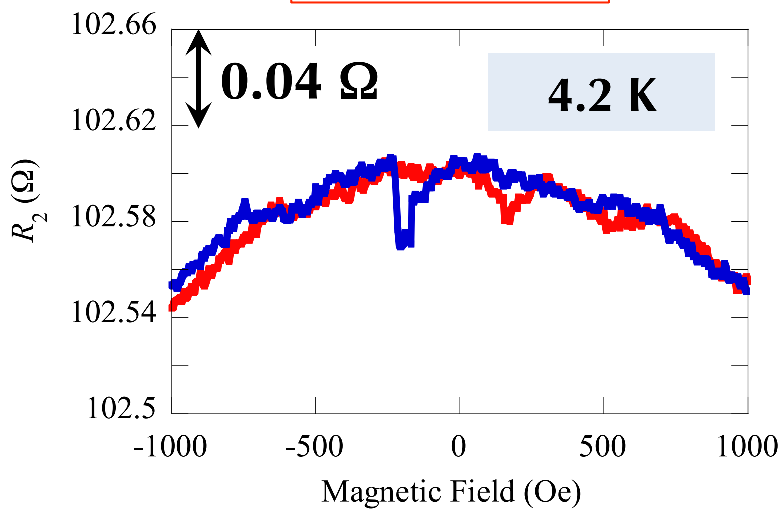

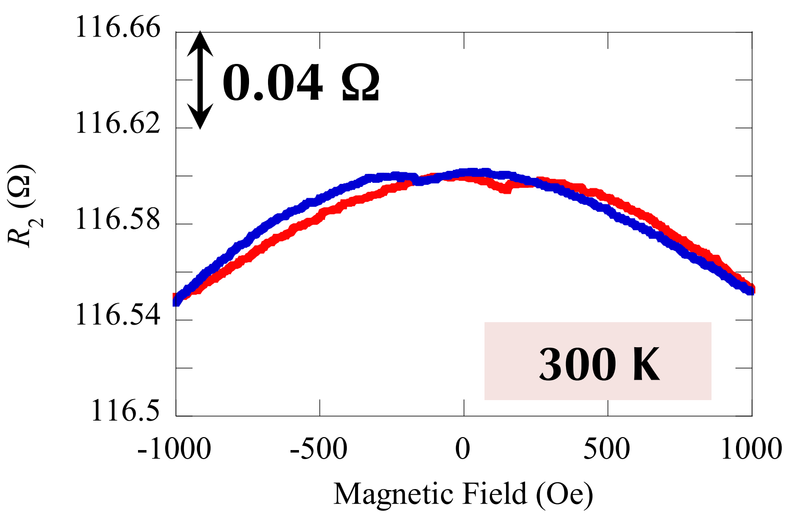

I =-100 mA

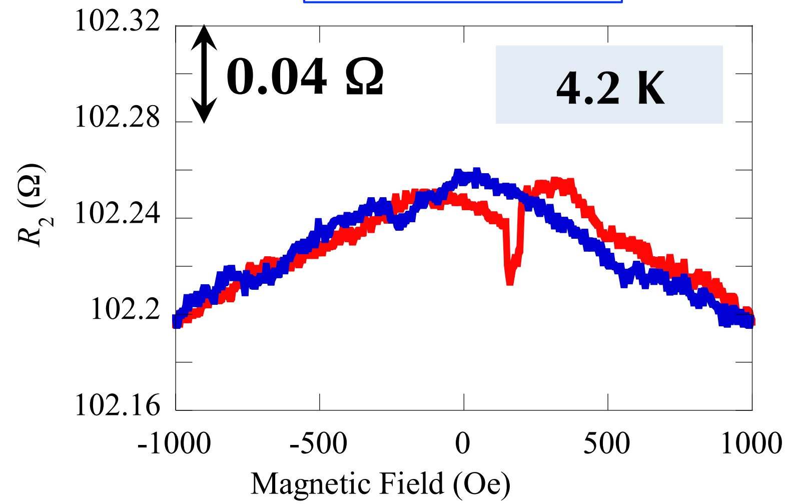

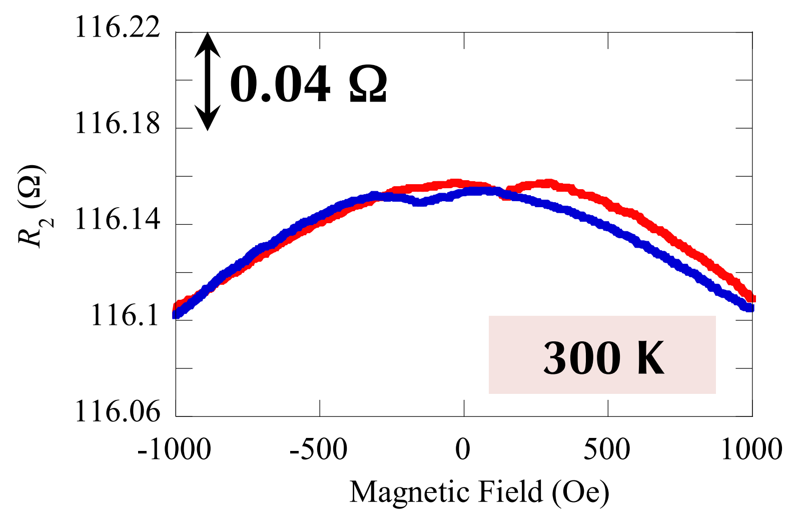

No rectangular hysteresis signals

Spin-charge coupled transport (theory & exp.)

Nano spin conversion

Magnetoresistance

$$V = -\frac{1}{e\rho(\epsilon_F)}\int_{-L/2}^{L/2}\frac{dN}{dx}dx = \frac{2\pi IL}{e^2k_F\ell} + \boxed{\frac{4\pi I\eta}{e^2k_F}}$$

Burkov et al., Phys. Rev. Lett. 105, 066802(2010).

100×10^{-6} [A=C/s]

1.05×10^{-34} [J･s=CV･s]

Spin polarization of injected current

$$V = \frac{4\pi I\hbar\eta}{e^2k_Fm}$$

Width of TI channel 2000 [nm] $=2\times10^4$ [Å]

1.60×10^{-19} [C]

0.05~0.1 $Å^{-1}$ from ARPES
(S. Kim et al., PRL. 112, 136802 (2014).)

This study: 2V=4～40μV⇒ η =0.05~0.5%

Nano-carbon

Single-layer graphene

R. Ohshima, A. Sakai, M.S. et al., APL 2014.
S. Dushenko, M.S. et al., PRL 2016.

Single-walled carbon nanotubes

E. Shigematsu, H. Nagano, M.S. et al., in prep.

SOI in graphene !?

Graphene : small spin-orbit interaction : 1-10 μV

S. Konschuh et al., PRB 2010.

D. Huertas-Hernando et al., PRB 2006.

20 folds enhancement by defects, ripples etc.…

D. Huertas-Hernando et al., PRB 2006.

A. Castro Neto et al., PRL 2009.

Giant enhancement of SOI in SLG

J. Balakrishnan, B. Oeziylmaz et al., Nature Comm. 2014.

/ CVD-grown on Cu ⇒ Cu adatoms

/ θ_{SHE} ~ 0.2 (!) (3-orders of magnitude enhancement)

SOI enhancement in graphene ?

Hydrogenation :

SOI in hydrogenated SLG, enhanced.

J. Balakrishnan, B. Oeziylmaz et al., Nature Phys. 2013.

SOI = 2.5 meV (!)

NO! Hydrogenated SLG allows good spin coherence.

M. Wojtaszek, B. van Wees et al., PRB(R), 2013.

?

Spin conversion in graphene

Nano spin conversion

R. Ohshima, M.S. et al., APL 2014.
SLG/YIG, no-gating.

APPLIED PHYSICS LETTERS **105**, 162410 (2014)

CrossMark

Observation of spin-charge conversion in chemical-vapor-deposition-grown single-layer graphene

Ryo Ohshima,[1,a)] Atsushi Sakai,[1,a)] Yuichiro Ando,[1,2] Teruya Shinjo,[2] Kenji Kawahara,[3] Hiroki Ago,[3] and Masashi Shiraishi[1,2]

[1]*Graduate School of Engineering Science, Osaka University, Toyonaka 560-8531, Japan*
[2]*Department of Electronic Science and Engineering, Kyoto University, Kyoto 615-8531, Japan*
[3]*Institute for Material Chemistry and Engineering, Kyushu University, Fukuoka 816-8508, Japan*

$\theta_{SHE} \sim 6e\text{-}7$

J. Mendez, A. Azevedo, S. Rezende et al., PRL 2015.
SLG/YIG, no-gating.

PRL **115,** 226601 (2015) PHYSICAL REVIEW LETTERS week ending 27 NOVEMBER 2015

Spin-Current to Charge-Current Conversion and Magnetoresistance in a Hybrid Structure of Graphene and Yttrium Iron Garnet

J. B. S. Mendes,[1,*] O. Alves Santos,[2] L. M. Meireles,[3] R. G. Lacerda,[3] L. H. Vilela-Leão,[4] F. L. A. Machado,[2] R. L. Rodríguez-Suárez,[5] A. Azevedo,[2] and S. M. Rezende[2]

[1]*Departamento de Física, Universidade Federal de Viçosa, 36570-900 Viçosa, Minas Gerais, Brasil*
[2]*Departamento de Física, Universidade Federal de Pernambuco, 50670-901 Recife, Pernambuco, Brasil*
[3]*Departamento de Física, Universidade Federal de Minas Gerais, 31270-901 Belo Horizonte, Minas Gerais, Brasil*
[4]*Núcleo Interdisciplinar de Ciências Exatas e Inovação Tecnológica, Universidade Federal de Pernambuco, 55002-970 Caruaru, Pernambuco, Brasil*
[5]*Facultad de Física, Pontificia Universidad Católica de Chile, Casilla 306, Santiago, Chile*

(Received 25 May 2015; published 25 November 2015)

The IREE governs the spin conversion !!??

Why IREE ?

"Spatial inversion symmetry is automatically broken…"

$$V_{\mathrm{SP}}(H) = R_N \frac{\omega\, e\theta_{\mathrm{SH}}\lambda_N w\, p_{xz}\, g_{\mathrm{eff}}^{\uparrow\downarrow}}{8\pi} \times \tanh(t_N/2\lambda_N)\left(\frac{h}{\Delta H}\right)^2 L(H-H_R)\cos\phi,$$

One might attempt to interpret the origin of the voltage in YIG/SLG with the same spin-pumping ISHE mechanism, as done in Ref. [47]. To apply Eq. (2) for YIG/SLG we consider $t_N/2\lambda_N \ll 1$, so that $V_{\mathrm{SP}} = (R_N f e\theta_{\mathrm{SH}} w p_{xz} g_{\mathrm{eff}}^{\uparrow\downarrow} t_N/8)(h/\Delta H)^2$. This expression does not depend on the spin diffusion length, as expected for a single atomic layer, but it requires that an effective thickness t_N is attributed SLG. With $R_N = 3400\ \Omega$, $g_{\mathrm{eff}}^{\uparrow\downarrow} \approx 4 \times 10^{17}\ \mathrm{m}^{-2}$ obtained from the FMR linewidth increase in YIG/SLG, $\theta_{\mathrm{SH}} = 0.2$ reported in Ref. [33] for CVD graphene grown on Cu foil, the SLG thickness that would give the measured voltage in Fig. 4(b), $V_{\mathrm{SP}} = 5\ \mu\mathrm{V}$, is $t_N = 2 \times 10^{-11}$ m. This is too small compared to any effective thickness ascribed to a single-layer graphene [48], which is certainly nonphysical. Thus, the spin-pump-

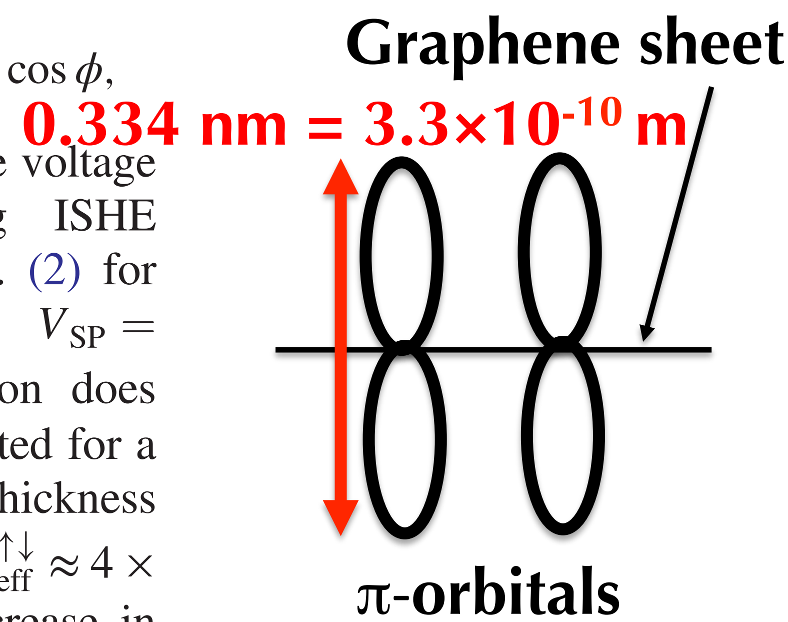

The precise investigation of SOI in graphene

PRL **116,** 166102 (2016) PHYSICAL REVIEW LETTERS week ending 22 APRIL 2016

Gate-Tunable Spin-Charge Conversion and the Role of Spin-Orbit Interaction in Graphene

S. Dushenko,[1,2] H. Ago,[3] K. Kawahara,[3] T. Tsuda,[4] S. Kuwabata,[4] T. Takenobu,[5] T. Shinjo,[2] Y. Ando,[2] and M. Shiraishi[2,*]
[1]*Graduate School of Engineering Science, Osaka University, Toyonaka 560-8531, Japan*
[2]*Department of Electronic Science and Engineering, Kyoto University, Kyoto 615-8510, Japan*
[3]*Institute for Material Chemistry and Engineering, Kyushu University, Fukuoka 816-8508, Japan*
[4]*Graduate School of Engineering, Osaka University, Suita 565-0871, Japan*
[5]*School of Advanced Science and Engineering, Waseda University, Tokyo 169-8555, Japan*
(Received 4 July 2015; revised manuscript received 19 November 2015; published 21 April 2016)

/ SLG (CVD-grown) on YIG
/ Ionic gating
//strong electric field applications
c.f.) K. Ueno et al., Nature Nanotech. 2011.
Gate-induced superconductivity in KTaO3
// Ambipolar spin conversion

Sample structure & SLG quality

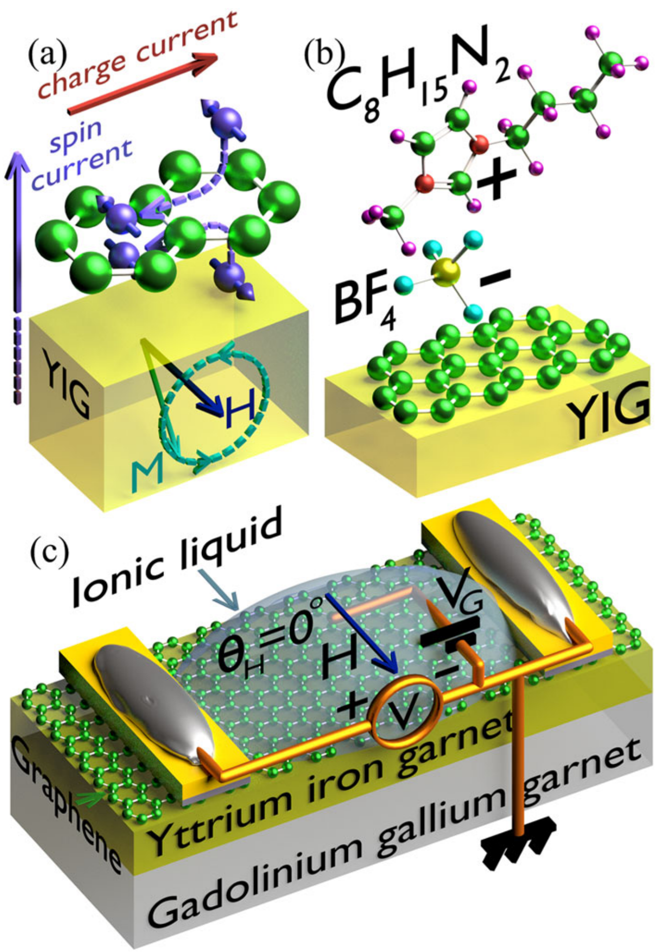

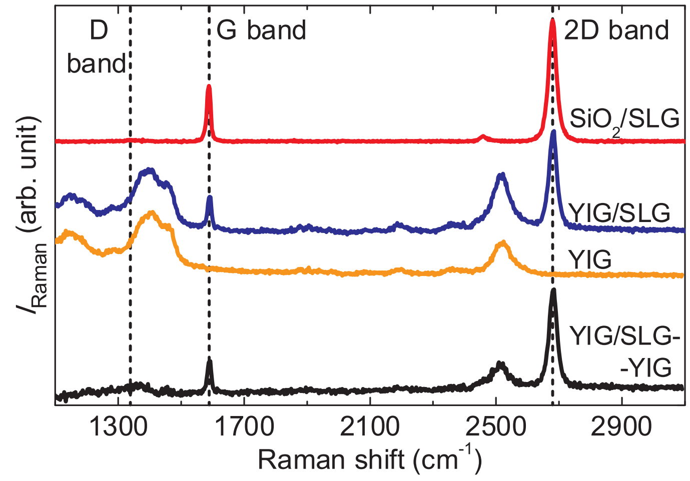

/ CVD-grown SLG on YIG

/ Cu adatoms : none

/ BF_4 + $C_8H_{15}N_2$
as an ionic liquid

/ Gating at 250 K

/ Spin pumping at 200 K
(9 GHz, 4 mW)

The precise investigation of SOI in graphene

Ambipolar FET

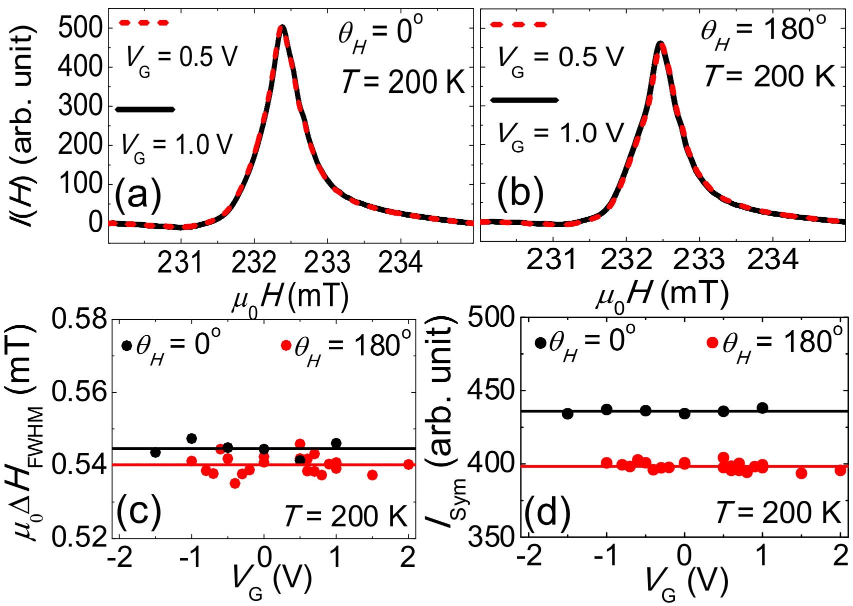

Gate dependence of FMR

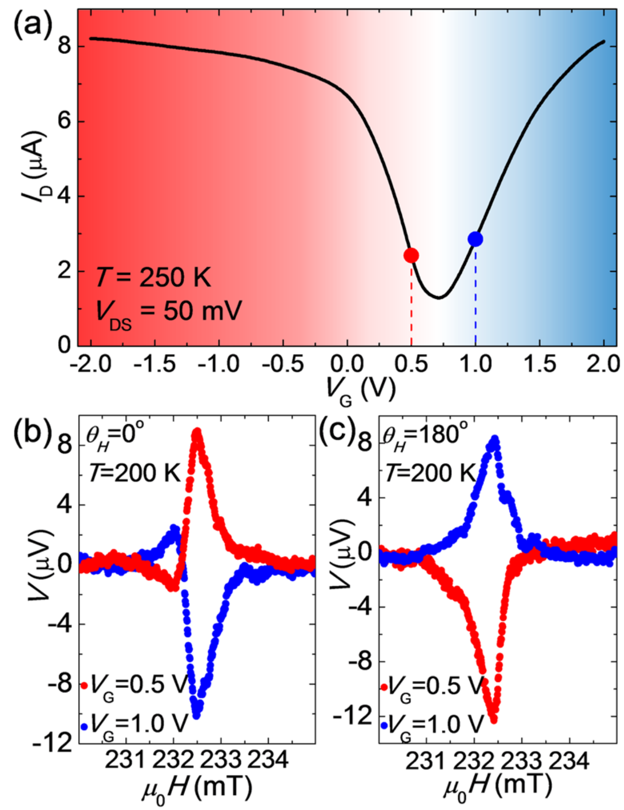

Ambipolar spin conversion

θ_{SHE} ~ 1e-7 (the SOI ~1.7 meV)

The precise investigation of SOI in graphene

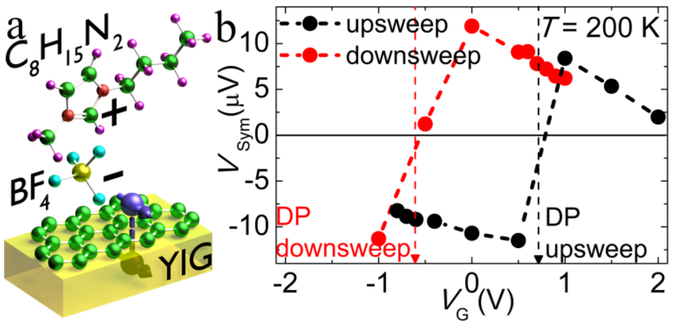

Gate-tunable EMFs

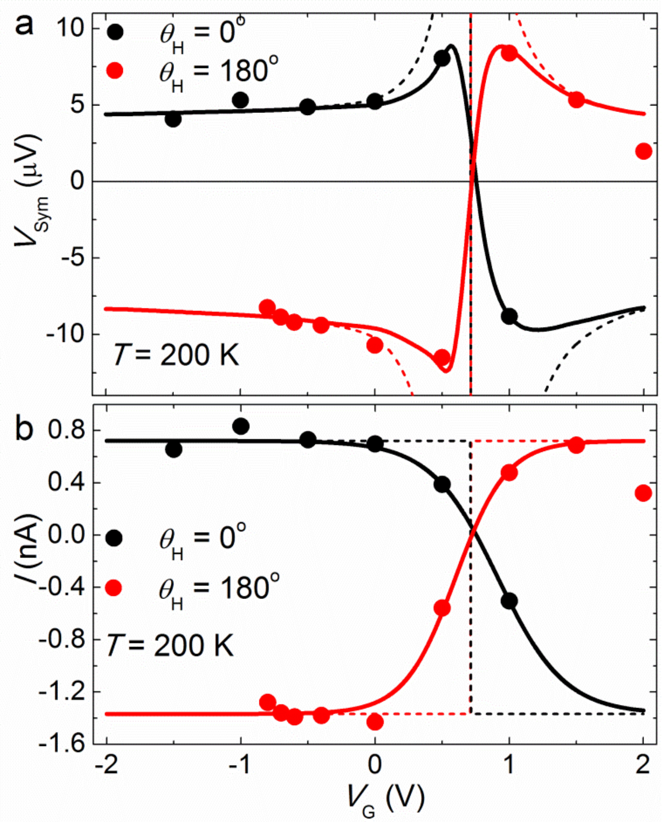

Dashed line : one-carrier model
Solid line : e-h puddle

Electron-hole puddle governs
the conversion at around the Dirac point.

I is not linearly dependent on V_g.

⇒ No IREE effect even in SLG.

New heating effect of YIG under the FMR

Investigation of the unidirectional spin heat conveyer effect in a 200nm thin Yttrium Iron Garnet film

O. Wid[1], J. Bauer[2], A. Müller[1], O. Breitenstein[2], S. S. P. Parkin[2], and G. Schmidt*[1,3]
[1]*Institut für Physik, Martin-Luther-Universität Halle-Wittenberg, Halle, 06120, Germany*
[2]*Max Planck Institute of Microstructure Physics, Halle, 06120, Germany*
[3]*IZM, Martin-Luther-Universität Halle-Wittenberg, Halle, 06120, Germany*
∗*Address for correspondence: georg.schmidt@physik.uni-halle.de*

arXiv:1602.01662

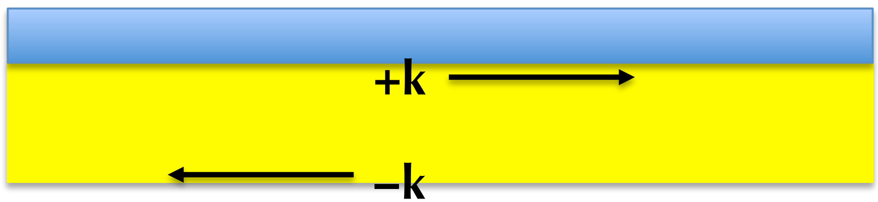

Thick (> 200 nm) YIG + conductive material

If +k and –k, different, the heat conveyer effect is !

⇒ Temperature difference at the both edges can induce an electromotive force due to the Seebeck effect of the conductor.

In our case, ΔT~2-3 mK & S=20~30 μV/K. ⇒ V < 100 nV (max.)

The measured EMFs in SLG & SWNTs comes from the ISHE !!

Negative spin Hall angle in solids

Indication of intrinsic spin Hall effect in 4*d* and 5*d* transition metals

M. Morota,[1] Y. Niimi,[1,*] K. Ohnishi,[1] D. H. Wei,[1] T. Tanaka,[2] H. Kontani,[2] T. Kimura,[1,†] and Y. Otani[1,3,‡]
[1]*Institute for Solid State Physics, University of Tokyo, 5-1-5 Kashiwa-no-ha, Kashiwa, Chiba 277-8581, Japan*
[2]*Department of Physics, Nagoya University, Furo-cho, Nagoya 464-8602, Japan*
[3]*RIKEN-ASI, 2-1 Hirosawa, Wako, Saitama 351-0198, Japan*

PRL **102,** 016601 (2009) PHYSICAL REVIEW LETTERS week ending 9 JANUARY 2009

Giant Orbital Hall Effect in Transition Metals: Origin of Large Spin and Anomalous Hall Effects

H. Kontani,[1] T. Tanaka,[1] D. S. Hirashima,[1] K. Yamada,[2] and J. Inoue[3]
[1]*Department of Physics, Nagoya University, Furo-cho, Nagoya 464-8602, Japan*
[2]*Ritsumeikan University, 1-1-1 Noji Higashi, Kusatsu, Shiga 525-8577, Japan*
[3]*Department of Applied Physics, Nagoya University, Furo-cho, Nagoya 464-8602, Japan*
(Received 29 May 2008; published 6 January 2009)

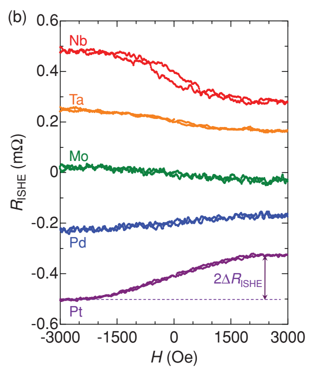

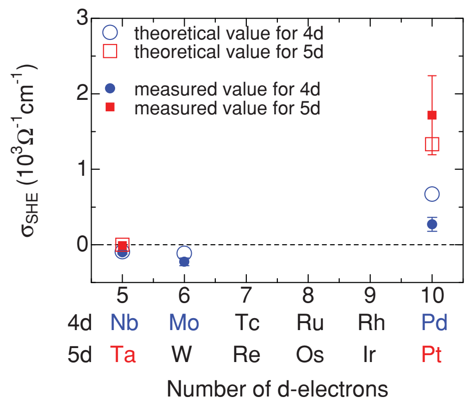

Negative spin Hall angle, θ_{SHE} : d-electron metals (before half filled)

The first material with negative θ_{SHE} except for 4d, 5d metals !!

Summary

/ Spin-orbitronics using
heavy (Bi)
light (C)
elements was discussed.

/ The interplay of the ISHE and the IREE
is quite attractive.